Joint Particle Filter and UKF Position Tracking in Severe Non-Line-Of-Sight Situations

Jose M. Huerta, Josep Vidal, Audrey Giremus, Jean-Yves Tourneret

Joint Particle Filter and UKF Position Tracking in Severe Non-Line-of-Sight Situations

Jose M. Huerta, Josep Vidal, *Member, IEEE*, Audrey Giremus, and Jean-Yves Tourneret, *Senior Member, IEEE*

***Abstract*—The performance of localization techniques in a wireless communication system is severely impaired by biases induced in the range and angle measures because of the non-line-of-sight (NLOS) situation, caused by obstacles in the transmitted signal path. However, the knowledge of the line-of-sight (LOS) or NLOS situation for each measure can improve the final accuracy. This paper studies the localization of mobile terminals (MT) based on a Bayesian model for the LOS-NLOS evolution. This Bayesian model does not require having a minimum number of LOS measures at each acquisition. A tracking strategy based on a particle filter (PF) and an unscented Kalman filter (UKF) is used both to estimate the LOS-NLOS situation and the MT kinetic variables (position and speed). The approach shows a remarkable reduction in positioning error and a high degree of scalability in terms of performance versus complexity.**

***Index Terms*—Non-line-of-sight (NLOS), particle filter, position measurement, Rao–Blackwellization, unscented Kalman filter.**

I. Introduction

GEOGRAPHICAL location in cellular networks has attained quite importance in the recent years [1]. For that purpose, localization using dedicated positioning systems, such as the Global Positioning System (GPS), is receiving an increasing attention in the literature. The localization is a human need and the possibility of developing related value-added services has promoted this field [2], [3]. The enhanced 911 (E911) services requirements [4] have led to the development of reliable localization systems in USA. Phase II of E911 imposes wireless communication systems a stringent location accuracy of 50 m for 67% of cases and 150 m for 95% of cases.

The elements involved in the radio localization are a mobile terminal (MT), which is to be located, and an undetermined number of known position nodes, called in this article anchor nodes (ANs). These ANs can be any transmitter or receiver like a GSM or UMTS base station (BS), a mobile phone, an access point (in wireless LAN) or a satellite (in GPS or Galileo) among others. The localization can be performed at uplink, where the ANs estimate the position from the received MT signals, or downlink, where the MT locates itself from signals transmitted by the ANs (as in GPS navigation). In both cases, the mobile localization is based on parameter estimates like time-of-arrival (TOA), time-difference-of-arrival (TDOA), signal strength (SS), angle-of-arrival (AOA), or others (see [5] for a complete review of the most common localization strategies). It has been theoretically demonstrated that localization based on parameters achieves the same accuracy as localization based on the received signals for the most common localization schemes [6]. The estimation accuracy for these parameters is of vital importance in the position calculation. A terminal tracker proceeds in two steps: 1) estimate some measures from the received signals; 2) use a position calculation function to estimate the MT position from these estimates.

It is well known that the greatest impairment to this estimation is the bias introduced by the non-line-of-sight (NLOS) condition masking all other error contributions when present [7]. It is even sometimes referred to as a killer issue, making corrupted measures useless [8]. In fact, many authors have considered that NLOS contaminated measures are not informative and should be discarded at the position calculation function if no prior information is available [9]. Also in this line, many works have been conducted to detect and discard these measures [10]. However, in real urban scenarios these strategies are not suitable since a high number of measures are contaminated by NLOS biases: normally an MS overhears four or five BSs in a GSM urban scenario. The majority of these BSs are in NLOS [11], thus leaving not enough suitable measures to perform an accurate localization. Another problem that arises is the classification of the line-of-sight (LOS) or NLOS condition. Some works are oriented in determining this condition from the received signal [12]. However, most studies estimate jointly the LOS-NLOS condition and the position at the position calculation function [10]. In this case, misclassification errors lead to an additional source of positioning inaccuracies. When localizing the MT under severe NLOS conditions (understand severe as a high likelihood of having NLOS at each measure) the number of ANs in LOS is not sufficient to apply detection/exclusion strategies. On its turn, it has been demonstrated both theoretically [6] and experimentally [13] that measures contaminated with NLOS are useful if prior knowledge about the NLOS error is available. This paper focuses on the design of a position calculation function that combines a particle filter (PF) with an unscented Kalman, filter (UKF) to track not only the MT position but also the LOS-NLOS situation. The rationale

J. M. Huerta and J. Vidal are with the Signal Processing and Communications Group (SPCOM), Technical University of Catalonia (UPC), 08034 Barcelona, Spain (e-mail: huerta@gps.tsc.upc.edu; josep.vidal@upc.edu).

A. Giremus is with the Signal and Image Processing Group, Laboratory IMS, University of Bordeaux, 33405 Talence, France (e-mail: audrey.giremus@laps.ims-bordeaux.fr).

J.-Y. Tourneret is with the ENSEEIHT-IRIT-TéSA, University of Toulouse, 31071 Toulouse cedex 7, France (e-mail: jean-yves.tourneret@enseeiht.fr).

for the combination of both trackers is the Rao–Backwellization strategy, which results in a considerable reduction of the computational cost when compared with classical PF solutions, and higher accuracy when compared with classical Kalman Filter (KF) solutions.

The paper is organized as follows. Section II reviews the current NLOS mitigation strategies. Section III states the objectives and assumptions. Section IV describes the dynamical model that governs the MT motion, the LOS-NLOS situation and the measurements. Section V presents two novel localization approaches, offering a tradeoff between accuracy and complexity. These approaches are compared to algorithms previously published in the literature through simulations described in Section VI. Conclusions are finally drawn in Section VII.

II. NLOS Impact Mitigation Strategies

This section reviews the current strategies for mitigating the NLOS impact on positioning which have been reported in the literature. These techniques are classified into different families for ease of reading.

A. Hypothesis Tests

With the objective of discarding or reducing the influence of NLOS on the final position estimation, it is possible to define a hypothesis test to decide which ANs are in LOS, given some kind of reliability measure. For that purpose, [10] defines a residual as the error between the actual measures and predicted measures from the estimated position under each hypothesis. The fraction of hypotheses with the highest residual is discarded. Then a final position is computed as the weighted average of the estimated positions under the remaining hypotheses (the weights being inversely proportional to the residual). The main flaw of this approach is that it does not take advantage of the fact that the NLOS biases are always positive. This flaw is alleviated in [14]. The work presented in [15], [16] combines the approach proposed in [10] with a maximum-likelihood (ML) closed-form solution. An extension to a dynamical location framework (where a trellis search is performed over the set of hypotheses) is presented in [17].

B. Statistical Analysis

The statistical analysis of the observations through time can improve the detection of NLOS situation. In [8] this information is used to estimate the bias introduced by the NLOS situation. It assumes constant bias, a very restrictive assumption that can only be taken for static MTs. The detection of NLOS using statistical information (in order to discard biased measures) was studied in [18]. This statistical information was combined with geometrical information in [19]. The ANs closer to the MT are considered more likely to be in LOS. The NLOS situation leads to a higher position estimation variance. Through the computation of prediction and observation errors, it is possible to discern between both situations [20], [21].

C. LOS-NLOS Tracking

The LOS-NLOS situation can be tracked to adapt the position estimator to this condition. A convenient method for that purpose is to track the bias introduced by NLOS situations. For a static MT, this bias can be considered as constant [8]. On the other hand, considering the bias as a random walk [22] makes it possible to track non-static MTs. Following this strategy, [23] estimates which measures are in NLOS prior to estimate the bias and [24], [25] uses a PF to track which measures incur a bias change. The LOS-NLOS situation can also be tracked by being modeled as a Markov process as in [21], [26].

D. Noise Models

All the works of this family are based on modeling the observation noise in a different fashion depending on the LOS-NLOS situation. One possibility is to consider that the observation noise variance and bias increases with NLOS condition [20], [23], [26]. In [27], a position estimator is developed considering Gaussian noise for LOS cases and exponential noise for NLOS cases. In [14], the idea of [10] is developed to discard all NLOS measures. If there are not enough LOS measures, the NLOS measures with less residual are included in the observation vector, but assuming they are contaminated by an asymmetric Gaussian noise.

E. Robust Parameter Estimation

This family of NLOS mitigation strategies is based on obtaining more information from the received signal using quality measures or directly estimating a reduced bias parameter. In [12] and [28], a scattering model is developed in order to identify the origin of scatter, which is directly related to the MT position. The TOA are estimated from the received signal as well as the multiple arrivals associated to multipath. Comparing the multipath distribution with the scattering model, one can infer the unbiased TOA. However, this approach is difficult to apply in practice because of the computational complexity resulting from the determination of all arrival times.

At GPS, most NLOS mitigation techniques consist of making the receiver estimation of the satellite signal propagation delays more robust to the presence of a NLOS delayed replica. For that purpose, new discriminator functions have been introduced such as for instance the Strobe and Enge correlator [29]. As an alternative, one can directly detect the measurement biases induced by multipath while solving the navigation problem. For that purpose, classical integrity monitoring techniques such as the multiple solution separation algorithm [30] can be applied even if they are first intended to satellite failure detection and identification. The main drawback of such techniques is that the biased parameters are excluded.

F. Our Contribution

The approaches presented in this paper share some characteristics with previous strategies. A hypothesis test, a statistical analysis and an LOS-NLOS tracking are inherent to the proposed PF. The idea of modeling the noise distributions differently under LOS-NLOS situations is also investigated. Finally, the proposed strategies could also be included among the robust parameter estimation techniques because of the use of quality measures. In addition, the proposed approaches take advantage of previously proposed strategies to cope with the NLOS effects. Using a Bayesian model, they fully exploit the LOS and

NLOS measurements and hence are able to perform satisfactorily on realistic scenarios. More precisely, they can be used in situations where not enough LOS measures are available, while maintaining an affordable computational complexity.

III. General Assumptions

The objective of this paper is to estimate the position of an MT using N measures originated from B ANs. Note that N and B are not necessarily equal since one AN may provide more than one measure, e.g., TOA and AOA, or one measure may come from two ANs, e.g., TDOA. The proposed scenario can be a mobile cellular network, a GPS (in this case only TOA measurements are available) or any radio system (like wireless or sensor networks). This includes hybrid systems, like an UMTS mobile phone equipped with a GPS, using both signals for self-localization. The proposed problem formulation is appropriate for uplink measures (at the ANs) or downlink measures (at the MT, using signals transmitted from the ANs). The measures can be TOA, relative TOA (RTOA) (also known as pseudo TOA or pseudoranges), uncorrelated TDOA or AOA. The correlated TDOA [31] are not considered in this paper since a better accuracy can be achieved when tracking using RTOA as demonstrated in Appendix A. The phase between antennas is considered for AOA-based positioning instead of the geometric angle of arrival because the noise is independent from the phase, but not from the angle of arrival. It is straightforward to extend the proposed approaches to other types of measures provided the observation noise is additive. Also, additional measures from sensors external to the system (such as an MT mounted inertiometer) can be considered.

The ANs can be reasonably assumed to be perfectly synchronized. Indeed GPS satellites are synchronized. Moreover, GSM and UMTS cellular networks with enhanced observation time difference or observed TDOA localization schemes are provided with some synchronization between ANs [5]. This paper covers two possibilities for MT synchronization. In the first one, the MT is synchronized with the AN network. In the second one, the most common, the MT clock reference is different from the ANs, meaning that a clock skew can exist between the MT and the ANs. Since the quartz clocks currently inside handhelds are imprecise for localization purposes, a clock drift will be present causing the clock skew to evolve over time.

Finally, we assume that signal quality measures are available at the receiver. These quality measures include signal-to-interference-and-noise ratio (SINR) or delay spread, and a prior probability of how they are related to the LOS-NLOS situation. This information can be obtained from a measurement campaign. For instance, a campaign performed in Barcelona (Spain) showed experimentally a correlation between the delay spread and the LOS-NLOS situation. The resulting delay spread distributions are depicted in Fig. 6. The considered scenario is urban resulting in high probability of NLOS, and does not assume a minimum number of ANs in LOS.

With the aim of avoiding the light speed factor in the equations *light meter* (lm) is used as time unit, where one lm is the time it takes to the light to travel one meter:

$$1\text{lm} = \frac{1}{c}\,\text{s}. \tag{1}$$

IV. Model

The system can be modeled using a Bayesian framework with the classical state $\mathbf{f}$ and observation $\mathbf{g}$ functions

$$\begin{aligned} \breve{\mathbf{x}}_t &= \mathbf{f}(\breve{\mathbf{x}}_{t-1}, \breve{\mathbf{u}}_t) \\ \breve{\mathbf{y}}_t &= \mathbf{g}(\breve{\mathbf{x}}_t, \breve{\mathbf{u}}_t) \end{aligned} \tag{2}$$

where $\breve{\mathbf{x}}_t$ is the state vector, $\breve{\mathbf{y}}_t$ is the observation vector, and $\breve{\mathbf{u}}_t$ and $\breve{\mathbf{n}}_t$ are noises. A deeper analysis of the functions $\mathbf{f}$ and $\mathbf{g}$ reveals that they are composed of both linear and nonlinear parts. With the aim of tracking the linear and nonlinear variables separately, the nonlinear parameters can be marginalized out yielding the following equations:

$$\begin{aligned} \mathbf{x}_t &= \mathbf{f}(\mathbf{x}_{t-1}, \mathbf{u}_t) \quad \mathbf{s}_t = \mathbf{h}(\mathbf{s}_{t-1}, \mathbf{v}_t) \\ \mathbf{y}_t &= \mathbf{g}(\mathbf{x}_t, \mathbf{n}_t, \mathbf{s}_t) \quad \mathbf{o}_t = \mathbf{l}(\mathbf{s}_t, \mathbf{w}_t) \end{aligned} \tag{3}$$

where the left-hand side equations are the state $\mathbf{f}(\cdot)$ and observation $\mathbf{g}(\cdot)$ of the kinetics variables stacked in the vector $\mathbf{x}_t$, $\mathbf{y}_t$ are the observations related to $\mathbf{x}_t$ which also depend on the LOS-NLOS situation $\mathbf{s}_t$. The right-hand side equations are the state $\mathbf{h}(\cdot)$ and observation $\mathbf{l}(\cdot)$ of the LOS-NLOS situation $\mathbf{s}_t$, $\mathbf{o}_t$ are the observations related to $\mathbf{s}_t$. $\mathbf{u}_t$, $\mathbf{n}_t$, $\mathbf{v}_t$, and $\mathbf{w}_t$ are noises. The detailed definitions of the terms involved in (3) are provided below.

A. State Evolution and Observations

Since the kinetic state equation is linear, the state and observation equations resulting from (3) can be written as

$$\begin{aligned} \mathbf{x}_t &= \mathbf{F}\mathbf{x}_{t-1} + \mathbf{u}_t \\ \mathbf{y}_t &= \mathbf{g}(\mathbf{x}_t) + \mathbf{n}_{t,\mathbf{s}_t} \end{aligned} \tag{4}$$

where $\mathbf{x}_t$ is the state vector containing the position and the velocity. Depending on the considered localization scheme, the state vector may also contain the clock skew between MT and ANs and its derivative

$$\begin{aligned} \mathbf{x}_t &= [\,\mathbf{p}_t^T \quad \dot{\mathbf{p}}_t^T\,]^T \quad \text{Synchronized MT} \\ \mathbf{x}_t &= [\,\mathbf{p}_t^T \quad \tau_t \quad \dot{\mathbf{p}}_t^T \quad \dot{\tau}_t\,]^T \quad \text{Unsynchronized MT} \end{aligned} \tag{5}$$

where $\mathbf{p}_t$ and τ_t stand for the position and clock skew, respectively, and the upper dot stands for derivative with respect to time. The position can be two or three dimensional and is expressed in Cartesian coordinates.

The additive noise $\mathbf{u}_t$ is zero-mean Gaussian with covariance matrix $\mathbf{Q}_\mathbf{u}$ defined as follows:

$$\begin{aligned} \mathbf{Q}_\mathbf{u} &= \begin{bmatrix} \mathbf{0} & \mathbf{0} \\ \mathbf{0} & \Delta t \sigma_v^2 \mathbf{I} \end{bmatrix} \quad \text{Synchronized MT} \\ \mathbf{Q}_\mathbf{u} &= \begin{bmatrix} \mathbf{0} & \mathbf{0} & \mathbf{0} \\ \mathbf{0} & \Delta t \sigma_v^2 \mathbf{I} & \mathbf{0} \\ \mathbf{0} & \mathbf{0} & \Delta t \sigma_\tau^2 \end{bmatrix} \quad \text{Unsynchronized MT} \end{aligned} \tag{6}$$

where Δt is the time interval between acquisitions, and σ_v^2 and σ_τ^2 are the variances of speed and clock skew. The transition matrix $\mathbf{F}$ is defined as:

$$\mathbf{F} = \begin{bmatrix} \mathbf{I} & \Delta t \mathbf{I} \\ \mathbf{0} & \mathbf{I} \end{bmatrix} \tag{7}$$

where the number of columns of $\mathbf{I}$ is half the length of $\mathbf{x}_t$. The vector $\mathbf{y}_t$ contains the set of N measurements obtained from the B ANs and $\mathbf{g}(\mathbf{x}_t)$ is the ideal noise free measurement whose

TABLE I
IDEAL OBSERVATION FUNCTIONS

Measure	$g_i(\mathbf{x}_t)$
TOA	$\|\mathbf{p}_t - \mathbf{q}_i\|$
RTOA	$\|\mathbf{p}_t - \mathbf{q}_i\| + \tau_t$
TDOA	$\|\mathbf{p}_t - \mathbf{q}_{i,1}\| - \|\mathbf{p}_t - \mathbf{q}_{i,2}\|$
AOA	$\psi(\measuredangle(\mathbf{q}_i - \mathbf{p}_t))$

For TOA and RTOA measures, it is considered that the transmission time has been subtracted, so they represent the trip time. The TDOA is only considered for the uncorrelated case, since the correlated one is treated as RTOA measures (see Appendix A).

$\mathbf{q}_i$, $\mathbf{q}_{i,1}$ and $\mathbf{q}_{i,2}$ are the positions of the AN associated with the ith measurement. $\measuredangle(\bullet)$ stands for the angle of the vector and $\psi(\bullet)$ is a function that obtains the electric phase from the geometric angle and depends of the array geometry.

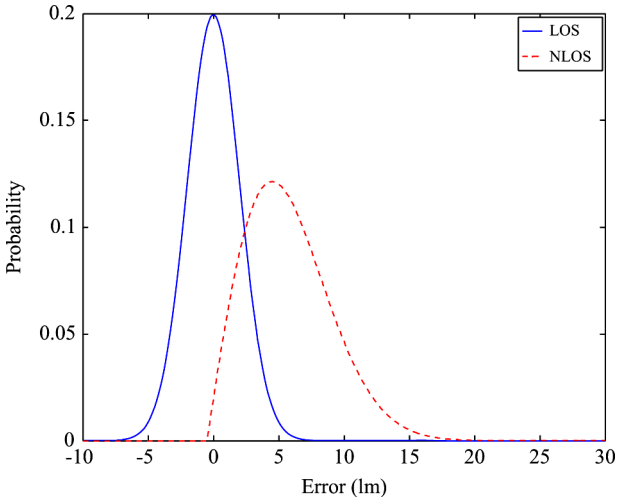

Fig. 1. Example of observation noise pdf depending of the LOS-NLOS situation for TOA and RTOA measures.

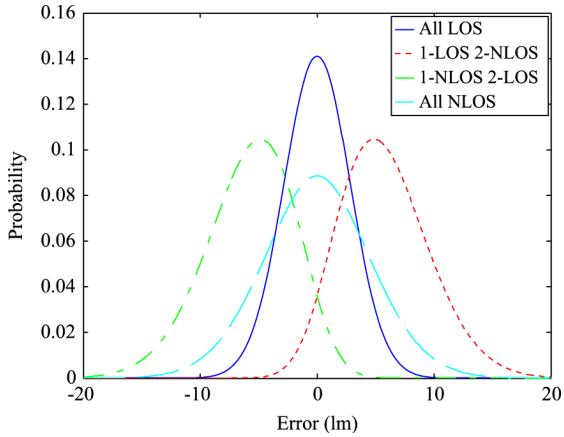

Fig. 2. Example of observation noise pdf for TDOA measures.

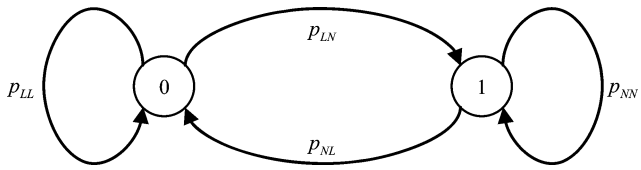

Fig. 3. Description of the states and transition probabilities for the situation MP.

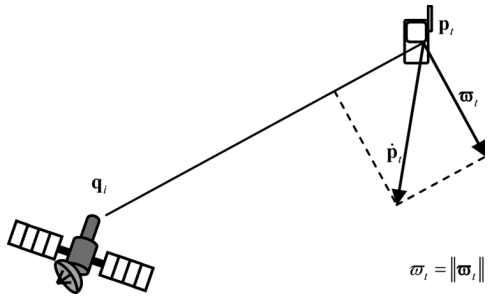

Fig. 4. Graphical definition of transversal speed ϖ_t.

elements are computed as described in Table I. The random vector $\mathbf{n}_t = [n_{1,t} \quad \cdots \quad n_{N,t}]^T$ has a probability density function (pdf) depending on the vector $\mathbf{s}_t = [s_{1,t} \quad \cdots \quad s_{B,t}]$, which contains the LOS-NLOS situation of each AN. Precisely, $s_{i,t} = 0$ for LOS and $s_{i,t} = 1$ for NLOS at AN i. For illustrative purposes, Fig. 1 shows an example of the noise pdf in presence or absence of NLOS bias for TOA and RTOA measurements. Fig. 2 depicts the noise pdf when TDOA are used and two ANs are involved (four possible situations have to be considered). In this case, the observation noise is the difference between the noises associated to the two ANs.

B. Situation Evolution

The situation vector $\mathbf{s}_t$ is modeled as evolving in time following a first-order Markov process (MP). Fig. 3 shows the possible transitions of this MP and the corresponding probabilities

$$\begin{aligned} p_{\mathrm{LL}} &= p(s_{i,t} = 0 | s_{i,t-1} = 0) \\ p_{\mathrm{LN}} &= p(s_{i,t} = 1 | s_{i,t-1} = 0) \\ p_{\mathrm{NL}} &= p(s_{i,t} = 0 | s_{i,t-1} = 1) \\ p_{\mathrm{NN}} &= p(s_{i,t} = 1 | s_{i,t-1} = 1). \end{aligned} \tag{8}$$

The components of the vector $\mathbf{s}_i$ are assumed to be mutually independent

$$p(\mathbf{s}_t | \mathbf{s}_{t-1}) = \prod_{i=1}^{B} p(s_{i,t} | s_{i,t-1}). \tag{9}$$

Let us assume that these probabilities are related to the MT transversal speed, i.e., the LOS-NLOS situation does not change when moving towards or away from the ANs. The transversal speed of an MT related to AN i is defined as

$$\varpi_{i,t} = \left\| \dot{\mathbf{p}}_t - \frac{(\mathbf{p}_t - \mathbf{q}_i)^T \dot{\mathbf{p}}_t}{\|\mathbf{p}_t - \mathbf{q}_i\|^2} (\mathbf{p}_t - \mathbf{q}_i) \right\| \tag{10}$$

which is the difference between $\dot{\mathbf{p}}_t$ and its projection on $\mathbf{p}_t - \mathbf{q}_t$, where $\mathbf{p}_t$ is the MT position, $\dot{\mathbf{p}}_t$ its velocity, and $\mathbf{q}_t$ denotes the ith AN position. The definition of the transversal speed is illustrated in Fig. 4.

It is possible to evaluate the time of remaining in a given state from the transition probabilities (8). Indeed, for an MT in NLOS situation, the probability of remaining k consecutive time instants in NLOS for AN i is

$$p(k|\mathrm{NLOS}) = p_{\mathrm{NL}}(1 - p_{\mathrm{NL}})^k. \tag{11}$$

Let us define n_{NLOS} as the number of consecutive time instants a terminal remains in NLOS and L_{NLOS} as the distance traveled by the MT in this interval (n_{LOS} and L_{LOS} denote the same quantities for the LOS case). The average of n_{NLOS} is given by

$$E\{n_{\mathrm{NLOS}}\} = \sum_{k=0}^{\infty} kp(k|\mathrm{NLOS}) = \frac{1-p_{\mathrm{NL}}}{p_{\mathrm{NL}}}. \quad (12)$$

Note that the duration of remaining in NLOS situation (in light meters) is related to the length of the NLOS state (in meters) through the MT transversal speed ϖ via

$$n_{\mathrm{NLOS}}\Delta t = \frac{L_{\mathrm{NLOS}}}{\varpi} \quad (13)$$

where Δt is the reference time interval at which transitions may occur (typically the sampling period of measures). Combining (12) with (13) yields

$$p_{\mathrm{NL}} = \frac{\varpi\Delta t}{\varpi\Delta t + E\{L_{\mathrm{NLOS}}\}} \quad (14)$$

a probability which is clearly time-varying as the speed changes with time. Analogously, the set of transition probabilities can be expressed as

$$\begin{aligned} p_{\mathrm{LL}} &= \frac{E\{L_{\mathrm{LOS}}\}}{\varpi\Delta t + E\{L_{\mathrm{LOS}}\}} \\ p_{\mathrm{LN}} &= \frac{\varpi\Delta t}{\varpi\Delta t + E\{L_{\mathrm{LOS}}\}} \\ p_{\mathrm{NL}} &= \frac{\varpi\Delta t}{\varpi\Delta t + E\{L_{\mathrm{NLOS}}\}} \\ p_{\mathrm{NN}} &= \frac{E\{L_{\mathrm{NLOS}}\}}{\varpi\Delta t + E\{L_{\mathrm{NLOS}}\}}. \end{aligned} \quad (15)$$

Therefore, if this model is used in a positioning environment, the average length (in meters) of the LOS and NLOS situations ($E\{L_{\mathrm{LOS}}\}$ and $E\{L_{\mathrm{NLOS}}\}$, respectively) are sufficient to characterize the environment (rural, suburban, urban, etc.). These average values should be determined for instance from a previous field campaign.

Note that the proposed model is valid only if $\varpi\Delta t \ll E\{L_{\mathrm{LOS}}, L_{\mathrm{NLOS}}\}$, i.e., when the probability of two transitions in one time interval is close to zero. Conversely, for $\varpi\Delta t \gg E\{L_{\mathrm{LOS}}, L_{\mathrm{NLOS}}\}$, $p_{\mathrm{NL}} \simeq p_{\mathrm{LN}} \simeq 1$, according to (15), which is obviously not satisfactory. Therefore, we need to generalize the model to high speeds or large sampling intervals. In particular, more than one transition inside a time interval has to be considered, requiring defining new transition probabilities. The transitions between LOS and NLOS situations (with probabilities p_{LN} and p_{LN}) are assumed instantaneous, and so, do not consume any time. Staying in the same situation (with probabilities p_{LL} and p_{NN}) is considered as a time *transition* consuming one time interval. Thus, each time interval is composed of an undetermined number of situation changes (p_{LN} and p_{NL}) and one time transition (p_{LL} and p_{NN}). A new set of probabilities consuming one time interval is therefore defined analogously to (8)

$$\begin{aligned} p'_{\mathrm{LL}} &= p(s_{i,t} = 0 | s_{i,t-1} = 0) \\ p'_{\mathrm{LN}} &= p(s_{i,t} = 1 | s_{i,t-1} = 0) \\ p'_{\mathrm{NL}} &= p(s_{i,t} = 0 | s_{i,t-1} = 1) \\ p'_{\mathrm{NN}} &= p(s_{i,t} = 1 | s_{i,t-1} = 1). \end{aligned} \quad (16)$$

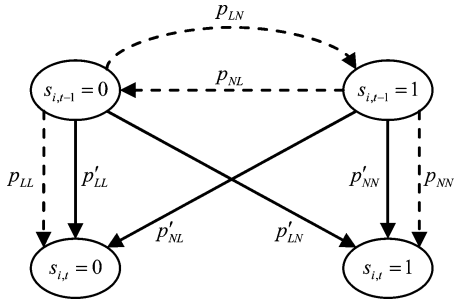

Fig. 5. MP description for the generalized evolution of the situation.

All these probabilities are graphically illustrated in Fig. 5 and their expressions are summarized as follows:

$$\begin{aligned} p'_{\mathrm{LL}} &= p_{\mathrm{LL}}\rho \quad p'_{\mathrm{LN}} = p_{\mathrm{LN}}p_{\mathrm{NN}}\rho \\ p'_{\mathrm{NL}} &= p_{\mathrm{NL}}p_{\mathrm{LL}}\rho \quad p'_{\mathrm{NN}} = p_{\mathrm{NN}}\rho \\ \rho &= \sum_{i=o}^{\infty} (p_{\mathrm{LN}}p_{\mathrm{NL}})^i = \frac{1}{1-p_{\mathrm{LN}}p_{\mathrm{NL}}}. \end{aligned} \quad (17)$$

Note that ρ is not a probability. The transition probabilities in (17) reduce to (15) for $\varpi\Delta t \gg E\{L_{\mathrm{LOS}}, L_{\mathrm{NLOS}}\}$. Conversely, for $\varpi\Delta t \ll E\{L_{\mathrm{LOS}}, L_{\mathrm{NLOS}}\}$, the transition probabilities can be written

$$\begin{aligned} p'_{\mathrm{LL}} &= p'_{\mathrm{NL}} = p_L = \frac{E\{L_{\mathrm{LOS}}\}}{E\{L_{\mathrm{LOS}}\} + E\{L_{\mathrm{NLOS}}\}} \\ p'_{\mathrm{NN}} &= p'_{\mathrm{LN}} = p_N = \frac{E\{L_{\mathrm{NLOS}}\}}{E\{L_{\mathrm{LOS}}\} + E\{L_{\mathrm{NLOS}}\}} \end{aligned} \quad (18)$$

where p_L and p_N are the probabilities obtained when no information about previous states is available (i.e., initial probabilities or without memory). In this last case, the tracking of the LOS-NLOS is completely useless. In order to avoid this problem, the selected value for Δt must satisfy $\Delta t \ll \min(E\{L_{\mathrm{LOS}}\}, E\{L_{\mathrm{NLOS}}\})/\nu_{\max}$, where $\nu_{\max}$ is the maximum MT speed.

C. Situation Observations

In parallel to the TOA measures, the proposed algorithm uses signal quality measures $\mathbf{o}_t$ that are somehow related to the LOS-NLOS situation. Some possible quality measures include SINR, delay spread, relation between expected and received power or geographical mapping. However, it is necessary to make the relationship between the observations and the situation vector explicit, i.e., to know $p(\mathbf{o}_t|\mathbf{s}_t)$. This knowledge can be obtained through a measurement campaign or by using some kind of adaptive strategy like the Baum–Welch algorithm [32]. A delay spread indicator (an example of situation observation) was obtained by the authors in [21] from a measurement campaign using real data. In this context, the delay spread indicator is determined as the relation between the signal to interference and noise ratio (SINR) of the detected incoming signal (the first arrival) and the SINR at the RAKE receiver. Equivalently, this indicator provides a relation between the power of the first arrival and the total received signal power, and thus a measure of multipath importance. We therefore assume that LOS situations correspond to an indicator value which is close to 1, whereas

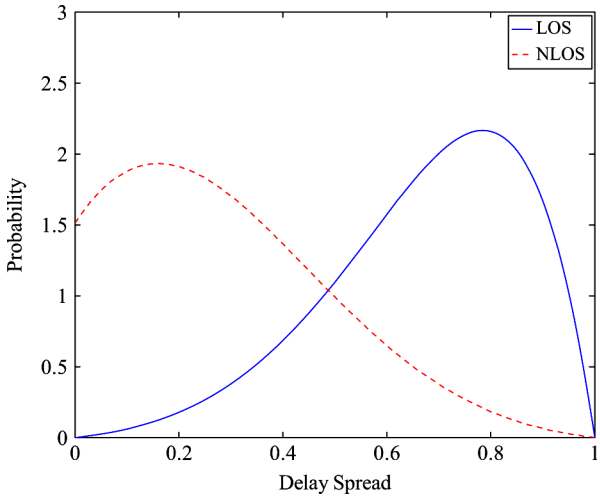

Fig. 6. PDF of the delay spread indicator conditional upon the LOS and NLOS situation for the associated BS (obtained empirically from real data).

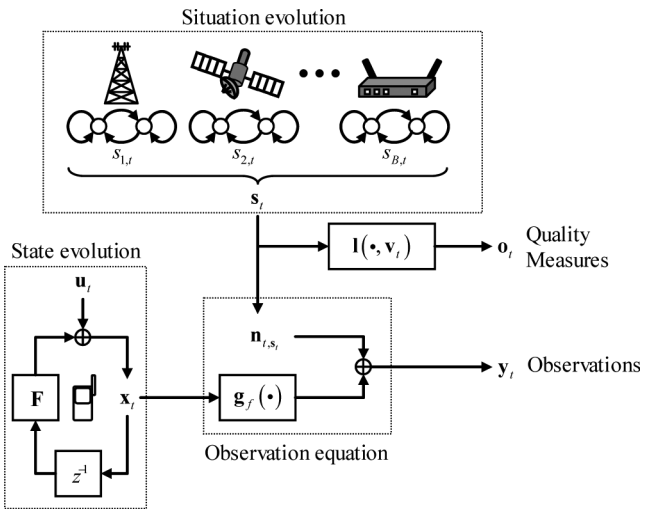

Fig. 7. State and situation model schematic.

a value close to 0 indicates NLOS situations. Fig. 6 depicts the pdf of the delay spread indicator for both LOS and NLOS cases.

D. General Overview

The complete system model is summarized in Fig. 7. The situation for each AN evolves independently from the other ANs according to an MP. The MT kinetics and clock skew (the state vector) vary over time as random walks. Two different sets of observations are available. The first observations, known as quality measures, only depend on the situation (LOS or NLOS). The other observations are obtained as a result of applying an observation function to the state and adding a noise whose statistics depends on the situation.

V. Estimation Method

We propose a Bayesian approach to estimate both the kinetic state vector $\mathbf{x}_t$ and the situation vector $\mathbf{s}_t$ from the observations $\mathbf{y}_{1:t}$ and quality measures $\mathbf{o}_{1:t}$ so as to benefit from *prior* information on the unknown parameters. In this framework, all inference is based on the posterior distribution $p(\mathbf{x}_t, \mathbf{s}_t|\mathbf{y}_{1:t}, \mathbf{o}_{1:t})$. As

TABLE II
Parameters Required to Characterize the Model

Parameter	Description
σ_v^2	Variance of speed
σ_r^2	Variance of clock skew
$\mathbf{g}(\cdot)$	Observation function
$p(\mathbf{n}\,\vert\,\mathbf{s})$	PDF of observation noise for each situation
$E\{L_{LOS}\}, E\{L_{NLOS}\}$	Mean distance travelled between situation changes
$p(\mathbf{o}\,\vert\,\mathbf{s})$	PDF of observation for each situation

the system model is highly nonlinear, PF's offer a convenient solution to this estimation problem as previously observed in [33] and [34]. In [35], linear systems whose parameters evolve according to a Markov chain are described as jump Markov linear systems and an efficient simulation-based algorithm is developed to recursively compute state estimates. This approach takes advantage of the fact that the model is conditionally linear Gaussian to solve analytically a part of the estimation problem. More precisely, only the Markov chain state is estimated by a PF, whereas the system state estimates are obtained by a KF. This algorithm is known as Rao–Blackwellized particle filter (RBPF) and has been shown to decrease the variance of the estimates. Although model (4) is nonlinear, a similar approach can be applied by using a UKF in place of the classical KF [13].

In the following, we describe two original algorithms to solve the localization issue in an NLOS environment. The first one is the RBPF whose steps have been reordered to decrease the computational complexity. In addition, efficient sampling strategies are proposed in accordance with the jump Markov system structure. The second algorithm, referred to as improved UKF (IUKF), assumes the LOS-NLOS situation only depends on the quality measures. In this way, the estimations of the kinetic states $\mathbf{x}_t$ and the situation vector $\mathbf{s}_t$ can be achieved separately. This method exhibits a lower computational complexity at the expense of reduced estimation accuracy.

In order to implement the proposed approaches some prior information is needed for the positioning system. The required priors are summarized in Table II.

A. The RBPF

An RBPF can be used when the state space model is linear Gaussian or almost linear Gaussian assuming a part of the state vector is known. For the problem at hand, the posterior distribution of interest can be factorized according to Bayes' rule

$$p(\mathbf{x}_t, \mathbf{s}_{1:t}|\mathbf{y}_{1:t}, \mathbf{o}_{1:t}) = p(\mathbf{x}_t|\mathbf{s}_{1:t}, \mathbf{y}_{1:t})\, p(\mathbf{s}_{1:t}|\mathbf{y}_{1:t}, \mathbf{o}_{1:t}). \tag{19}$$

Note that all the information about $\mathbf{s}_{1:t}$ and $\mathbf{x}_t$ is present in the posterior (19). According to this expression, the distribution $p(\mathbf{x}_t|\mathbf{y}_{1:t}, \mathbf{s}_{1:t})$ can be estimated by an EKF or a UKF, the latter being the strategy favored in this paper. The proposed RBPF algorithm thus combines a PF to generate samples according to $p(\mathbf{s}_{1:t}|\mathbf{y}_{1:t}, \mathbf{o}_{1:t})$ and a bank of UKF's to compute estimates of the kinetic states $\mathbf{x}_t$ conditionally upon the possible values of the situation vector $\mathbf{s}_t$. The PF and UKF used in this paper are classical (the reader is invited to consult [30], [31], [37], and[38]

for more details). The main steps required for the PF and UKF implementations are briefly recalled hereafter.

1) PF Estimation of the Situation Vector Distribution: PF are sequential techniques to deal with nonlinear and/or non-Gaussian problems that compute recursively a Monte Carlo approximation of the distribution of interest in the form

$$\hat{p}\left(\mathbf{s}_{1:t}|\mathbf{y}_{1:t},\mathbf{o}_{1:t}\right)=\sum_{i=1}^{M}\omega_t^{(i)}\delta\left(\mathbf{s}_{1:t}-\mathbf{s}_{1:t}^{(i)}\right) \tag{20}$$

where $\delta(\cdot)$ is the Dirac delta function and the support points $\mathbf{s}_{1:t}^{(i)}$, with associated weights $\omega_t^{(i)}$, are called particles. They are classically obtained by simulation according to the sequential importance sampling (SIS) technique whose principle is briefly recalled below. Ideally, the particles should be distributed according to the distribution of interest $p(\mathbf{s}_{1:t}|\mathbf{y}_{1:t},\mathbf{o}_{1:t})$. However, since it is usually impossible to sample according to this distribution, particles are propagated sequentially according to a proposal distribution $\pi(\cdot)$. The importance weights $\omega_t^{(i)}$ act as a correction for the discrepancy between $p(\cdot)$ and $\pi(\cdot)$

$$\omega_t^{(i)}\propto\frac{p\left(\mathbf{s}_{1:t}^{(i)}|\mathbf{y}_{1:t},\mathbf{o}_{1:t}\right)}{\pi\left(\mathbf{s}_{1:t}^{(i)}|\mathbf{y}_{1:t},\mathbf{o}_{1:t}\right)}. \tag{21}$$

The choice of the proposal distribution is crucial for an efficient implementation of the PF. However, since $\mathbf{s}_t$ takes values in a finite set, the most efficient strategy consists of directly exploring all the possible values of the situation vector. This results in a so-called deterministic PF presented for instance in [36]. Suppose that, at time t, the approximation of the posterior distribution is

$$\hat{p}\left(\mathbf{s}_{1:t-1}|\mathbf{y}_{1:t-1},\mathbf{o}_{1:t-1}\right)=\sum_{i=1}^{M}\omega_t^{(i)}\delta\left(\mathbf{s}_{1:t-1}-\mathbf{s}_{1:t-1}^{(i)}\right). \tag{22}$$

Since the number of possible offspring per particle amounts to 2^B, this approximation can be updated in an exhaustive manner as follows:

$$\hat{p}\left(\mathbf{s}_{1:t}|\mathbf{y}_{1:t},\mathbf{o}_{1:t}\right)=\sum_{i=1}^{M}\sum_{k=1}^{2^B}\omega_t^{(i,k)}\delta\left(\mathbf{s}_{1:t}-\mathbf{s}_{1:t}^{(i,k)}\right) \tag{23}$$

where $\mathbf{s}_{1:t}^{(i,k)}=\{\mathbf{s}_{1:t-1}^{(i)},\mathbf{s}_t^{(i,k)}=\mathbf{s}^{[k]}\}$ and $\mathbf{s}^{[k]}$ stands for the kth possible value of the situation vector. In this case, the importance weights are directly proportional to the posterior distribution of the particles

$$\omega_t^{(i,k)}\propto p\left(\mathbf{s}_{1:t}^{(i,k)}\middle|\,\mathbf{y}_{1:t},\mathbf{o}_{1:t}\right). \tag{24}$$

As a result, they can be factorized as follows:

$$\begin{aligned}\omega_t^{(i,k)}\propto\omega_{t-1}^{(i,k)}&p\left(\mathbf{s}_t^{(i,k)}|\mathbf{s}_{t-1}^{(i,k)}\right)\\&\times p\left(\mathbf{y}_t|\mathbf{s}_{1:t}^{(i,k)},\mathbf{y}_{1:t-1}\right)p\left(\mathbf{o}_t|\mathbf{s}_t^{(i,k)}\right).\end{aligned} \tag{25}$$

In this equation, the likelihood $p\left(\mathbf{y}_t|\mathbf{s}_{1:t}^{(i,k)},\mathbf{y}_{1:t-1}\right)$ is obtained from the UKF associated to particle $\mathbf{s}_{1:t}^{(i,k)}$. This approach has the advantage of not discarding any information. However, the number of particles is multiplied by 2^B at each step of the algorithm. In order to prevent an exponential increase of the computational complexity, a selection step must be applied. The easiest solution consists of maintaining only the M particles with the highest importance weights. More elaborated approaches can be implemented as detailed later.

2) Estimation of the Kinetic States: Even for a known $\mathbf{s}_{1:t}$, the system model (4) is nonlinear and possibly non-Gaussian in NLOS condition. Consequently, a standard KF cannot be applied to estimate the unknown state vector. The EKF [37], which is based on a first-order approximation of the nonlinearities, is classically used in this context [23], [38]. However, this algorithm is known to experience divergence when the state model is not accurate enough. Lately, the UKF was presented [39] as an alternative which yields more accurate state estimates than the EKF with a similar computational cost. As the EKF, the UKF provides a Gaussian approximation of the posterior pdf of the state vector given the measurements

$$\hat{p}\left(\mathbf{x}_{t-1}|\mathbf{s}_{1:t-1}^{(i,k)},\mathbf{y}_{1:t-1}\right)=\mathcal{N}\left(\bar{\mathbf{x}}_{t-1|t-1}^{(i,k)},\mathbf{Q}_{\mathbf{x}_{t-1|t-1}}^{(i,k)}\right) \tag{26}$$

where:

- $\mathbf{x}_{t|t}^{(i,k)}=E\{\mathbf{x}_t|\mathbf{s}_{1:t}^{(i,k)},\mathbf{y}_{1:t}\}$ is the state estimate;
- $\mathbf{Q}_{\mathbf{x}_{t|t}}^{(i,k)}$ is the covariance matrix of the UKF estimation error.

Contrary to EKF, UKF does not perform any approximation on the state space model but directly estimates the state distribution using the Unscented Transformation (UT). The UT is a deterministic sampling method to characterize a random variable which undergoes a nonlinear transformation. The UT represents the distribution of the random variable by a set of sigma points chosen deterministically. These sigma points can be propagated through the nonlinear function and therefore be used to capture the statistics of the output. There are several strategies to spread the sigma points. This paper uses the classical algorithm initially proposed in [40], [41] and recalled in Appendix B.

In the considered system, the UKF vector is composed not only of the kinetic states $\mathbf{x}_t$ but also of the measurement noise vector $\mathbf{n}_t$ since $p(\mathbf{n}_t|\mathbf{s}_{1:t})$ varies with time t and is not necessarily Gaussian. According to the UT, the set of sigma points corresponding to this random variable (RV) are propagated through the state and measurement equations. The classical KF equations are then applied to update the state estimate and its associate covariance matrix on the basis of the first- and second-order statistics obtained from the UT transform. This is the classical UKF whose algorithm is summarized in Table III, where $\mathcal{N}_{\mathbf{s}_t^{(i,k)}}$, in (III.1), is the sigma set associated with $\mathbf{n}_t$ for situation $\mathbf{s}_t^{(i,k)}$. The probability $p(\mathbf{y}_t|\mathbf{s}_{1:t}^{(i,k)},\mathbf{y}_{1:t-1})$ needed to evaluate (25), is obtained in (III.2). Finally, the posterior distribution of the kinetic states can be approximated by a mixture of Gaussian distribution according to Bayes' rule

$$p\left(\mathbf{x}_t\,|\mathbf{s}_{1:t},\mathbf{y}_{1:t}\right)=\sum_{k=1}^{2^B}\sum_{i=1}^{M}\omega_t^{(i,k)}\hat{p}\left(\mathbf{x}_t\,\middle|\,\mathbf{s}_{1:t}^{(i,k)},\mathbf{y}_{1:t}\right). \tag{27}$$

TABLE III
UKF ALGORITHM FOR RB APPROACH

- Calculate the sigma set:
  $\left\langle \overline{\mathbf{x}}_{t-1}^{(i)}, \mathbf{Q}_{\mathbf{x}_{t-1}}^{(i)} \right\rangle \xrightarrow{UT} \boldsymbol{\mathcal{X}}_{t-1}^{(i)}$
- Predict the state:
  $\boldsymbol{\mathcal{X}}_{t|t-1}^{(i)} = \mathbf{F}\boldsymbol{\mathcal{X}}_{t-1}^{(i)} + \boldsymbol{\mathcal{U}}$
  $\boldsymbol{\mathcal{X}}_{t|t-1} \xrightarrow{UT^{-t}} \left\langle \overline{\mathbf{x}}_{t|t-1}, \mathbf{Q}_{\mathbf{x}_{t|t-1}} \right\rangle$
- Predict the observation
  $\boldsymbol{\mathcal{Y}}_{t|t-1}^{(i)} = \mathbf{g}\left(\boldsymbol{\mathcal{X}}_{t|t-1}^{(i)}\right) + \boldsymbol{\mathcal{N}}_{\mathbf{s}_t^{(i)}}$ (III.1)
  $\boldsymbol{\mathcal{Y}}_{t|t-1}^{(i)} \xrightarrow{UT^{-1}} \left\langle \overline{\mathbf{y}}_{t|t-1}^{(i)}, \mathbf{Q}_{\mathbf{y}_{t|t-1}}^{(i)} \right\rangle$
- Obtain the Kalman Gain Matrix
  $\left\langle \boldsymbol{\mathcal{X}}_{t|t-1}^{(i)}, \boldsymbol{\mathcal{Y}}_{t|t-1}^{(i)} \right\rangle \xrightarrow{UT^{-t}} \mathbf{Q}_{\mathbf{xy}_{t|t-1}}^{(i)}$
  $\mathbf{K}_t^{(i)} = \mathbf{Q}_{\mathbf{xy}_{t|t-1}}^{(i)} \left(\mathbf{Q}_{\mathbf{y}_{t|t-1}}^{(i)}\right)^{-1}$
  $\overline{\mathbf{x}}_t^{(i)} = \mathbf{x}_{t|t-1}^{(i)} + \mathbf{K}_t^{(i)}\left(\mathbf{y}_t - \overline{\mathbf{y}}_{t|t-1}^{(i)}\right)$
  $\mathbf{Q}_{\mathbf{x}_t}^{(i)} = \mathbf{Q}_{\mathbf{x}_{t|t-1}}^{(i)} - \mathbf{K}_t^{(i)}\mathbf{Q}_{\mathbf{y}_{t|t-1}}^{(i)}\left(\mathbf{K}_t^{(i)}\right)^{-1}$
- Compute the probability of observation
  $\mathbf{g}\left(\boldsymbol{\mathcal{X}}_{t|t-1}^{(i)}\right) \xrightarrow{UT^{-1}} \tilde{\mathbf{y}}_{t|t-1}^{(i)}$
  $p\left(\mathbf{y}_t \mid \mathbf{s}_{1:t}^{(i)}, \mathbf{y}_{1:t-1}\right) = p\left(\mathbf{n}_t = \left(\mathbf{y}_t - \tilde{\mathbf{y}}_{t|t-1}^{(i)}\right) \mid \mathbf{s}_t^{(i)}\right)$ (III.2)

TABLE IV
RBPF ITERATION

- Propagate $\mathcal{S}_{t-1}$ to $\mathcal{S}_t'$, where each particle is propagated to cover all possible cases of $\mathbf{s}_t$.
  $\mathcal{S}_{t|t-1} = \{\forall \mathbf{s}_t\} \cdot \mathcal{S}_{t-1}$
- Run an UKF for each particle
  $\left\langle \overline{\mathbf{x}}_{t-1}^{(i)}, \mathbf{Q}_{\mathbf{x}_{t-1}}^{(i)}, \mathbf{s}_t^{(i)} \right\rangle \xrightarrow{UKF} \left\langle \overline{\mathbf{x}}_t^{(i)}, \mathbf{Q}_{\mathbf{x}_t}^{(i)}, p\left(\mathbf{y}_t \mid \mathbf{s}_{1:t}^{(i)}, \mathbf{y}_{1:t-1}\right) \right\rangle$ (IV.1)
- Update the weights
  $\omega_t^{(i)} \propto \omega_{t-1}^{(i)} p\left(\mathbf{s}_t^{(i)} \mid \mathbf{s}_{t-1}^{(i)}\right) p\left(\mathbf{y}_t \mid \mathbf{s}_t^{(i)}, \mathbf{y}_{1:t-1}\right) p\left(\mathbf{o}_t \mid \mathbf{s}_t^{(i)}\right)$
- Merge and select particles
  $\mathcal{S}_{t|t-1} \longrightarrow \mathcal{S}_t$

The state estimate can thus be computed as the weighted average of the UKF outputs

$$\hat{\mathbf{x}}_t = \sum_{k=1}^{2^B} \sum_{i=1}^{M} \omega_t^{(i,k)} \mathbf{x}_{t|t}^{(i,k)}. \tag{28}$$

3) Resampling: Once the UKFs have been run, it is possible to update the weights according to (25). In order to reduce the number of particles from $M \times 2^B$ to M, a straightforward solution would consist of preserving only the M particles with the most significant weight. This choice leads to particle degeneration, a situation where most of the particles carry the same information. A strategy is proposed instead, based on merging, which take advantage of the discrete of the situation vector. Suppose some particles have the same LOS or NLOS current situation and exhibit similar values for the kinetic vector $\mathbf{x}_t$. They do not bring additional information one from another, hence it suffices to maintain one of them, preferably the one with the highest weight. Consequently, before selecting the most likely particles, we introduce a merging step whose principle is described below.

The following distance is used to determine how close to each other two particles are:

$$d\left(\mathbf{s}_{1:t}^{(a)}, \mathbf{s}_{1:t}^{(b)}\right) = \begin{cases} \left\| \overline{\mathbf{x}}_t^{(a)} - \overline{\mathbf{x}}_t^{(b)} \right\| & \text{if } \mathbf{s}_t^{(a)} = \mathbf{s}_t^{(b)} \\ \infty & \text{if } \mathbf{s}_t^{(a)} \neq \mathbf{s}_t^{(b)} \end{cases} \quad \omega_t^{(a)} > \omega_t^{(b)} \tag{29}$$

where the standard L^2 norm $\|\cdot\|$ has been used. Note however that any weighted norm might also be applied since all components of $\mathbf{x}_t$ are expressed in similar units (m, m/s and lm). If the distance between two particles is lower than an appropriate threshold $d_{\min}$, the weights are recomputed as:

$$\begin{aligned} \omega_t^{(a)} &\longrightarrow \omega_t^{(a)} + \omega_t^{(b)} \\ \omega_t^{(b)} &\longrightarrow 0 \end{aligned} \tag{30}$$

which is equivalent to delete particle b and add its weight to particle a. This approach consists of forgetting the past and favoring the latest value of the situation vector in a similar manner as the selection step of the interacting multiple model algorithm [42]. The optimal threshold value depends on the situation transition probabilities, observation noise and number of particles. Lower values of the threshold reduce the protection against degeneration. A side effect of particle degeneration is to decide about the current situation at an early stage, thus increasing the probability of error in the classification. Also, a reduced number of particles increase the impairments of degeneracy. Otherwise, high values of the threshold (of the order of the minimum variance of the estimator output) degrade the accuracy, since the target density function is not well approximated by the PF. Experimentally, as a rule of thumb, we have observed that an appropriate value of $d_{\min}$ is

$$d_{\min} \simeq \frac{\sigma^2_{\|\hat{\mathbf{p}}-\mathbf{p}\|}}{10M} \tag{31}$$

where $\sigma^2_{\|\hat{\mathbf{p}}-\mathbf{p}\|}$ is the variance of the position estimator and M the number of particles. Bigger values of $\sigma^2_{\|\hat{\mathbf{p}}-\mathbf{p}\|}$ increase the threshold and reduce particle degeneration. Lower values decrease the threshold and increase accuracy. Moreover, the higher the number of particles M, the greater protection to degeneration. Once this merging rule has been applied to the complete set of particle, a classical pruning is carried out to obtain a set of M particles corresponding to the ones with the highest weights. The complete RBPF iteration is summarized in Table IV.

B. Reordered RBPF

The RBPF presented above needs the running of $M \times 2^B$ UKF to complete a recursion and propagates M particles to the next time step. It is possible to reduce the number of UKF down to M by simply reordering the RBPF steps, at the cost of a somewhat less relevant resampling. Prior to the UKF step (IV.1), it is possible to make use of the information brought by the quality

TABLE V
REORDERED RBPF ITERATION

- Propagate $\mathcal{S}_{t-1}$ to $\mathcal{S}_t'$, where each particle is propagated to cover all possible cases of $\mathbf{s}_t$.
  $\mathcal{S}_{t|t-1} = \{\forall \mathbf{s}_t\} \cdot \mathcal{S}_{t-1}$
- Update the weights
  $\omega_{t|t-1}^{(i)} \propto \omega_{t-1}^{(i)} p\left(\mathbf{s}_t^{(i)} \,|\, \mathbf{s}_{t-1}^{(i)}\right) p\left(\mathbf{o}_t \,|\, \mathbf{s}_t^{(i)}\right)$
- Merge and select particles
- Run an UKF for each particle
  $\left\langle \overline{\mathbf{x}}_{t-1}^{(i)}, \mathbf{Q}_{\mathbf{x}_{t-1}}^{(i)}, \mathbf{s}_t^{(i)} \right\rangle \xrightarrow{UKF} \left\langle \overline{\mathbf{x}}_t^{(i)}, \mathbf{Q}_{\mathbf{x}_t}^{(i)}, p\left(\mathbf{y}_t \,|\, \mathbf{s}_{1t}^{(i)}, \mathbf{y}_{1t-1}\right) \right\rangle$
- Update the weights
  $\omega_t^{(i)} \propto \omega_{t|t-1}^{(i)} p\left(\mathbf{y}_t \,|\, \mathbf{s}_t^{(i)}, \mathbf{y}_{1t-1}\right)$

measures to partially update the weights of the new particles according to

$$\omega_{t|t-1}^{(i,k)} \propto \omega_{t-1}^{(i,k)} p\left(\mathbf{s}_t^{(i,k)} | \mathbf{s}_{t-1}^{(i,k)}\right) p\left(\mathbf{o}_t | \mathbf{s}_t^{(i,k)}\right). \quad (32)$$

Then, the resampling process can be performed prior to the UKF according to these weights so that the number of particles is decreased to M before running the parallel UKF. After the UKF stage, the weights are finally updated as

$$\omega_t^{(i)} \propto \omega_{t|t-1}^{(i)} p\left(\mathbf{y}_t | \mathbf{s}_{1:t}^{(i)}, \mathbf{y}_{1:t-1}\right) \quad (33)$$

for $i = 1, \ldots, M$. The complete algorithm is detailed in Table V.

C. Improved UKF (IUKF)

Even with the reordering step, the RBPF solution requires a bank of UKF, hence is costly for a real time implementation. In this section, we propose a low complexity algorithm, called IUKF, using a simplifying assumption. It consists of estimating the situation vector by using only the information from the quality measures. In this way, the overall estimation problem is split into two independent problems of lower dimensions. In a first step, the quality measures are used to update the probabilities for the ANs to be in a given LOS-NLOS situation, $p(\mathbf{s}_{1:t}|\mathbf{o}_{1:t})$. Then, the obtained probabilities are incorporated to a modified UKF dedicated to the estimation of the continuous kinetic states conditionally to the LOS-NLOS environment.

1) Situation Estimator: This estimator considers, for the sake of simplicity, that the LOS-NLOS situations are independent between ANs and depend only on the situation observations

$$p\left(\mathbf{s}_{1:t} \,|\mathbf{y}_{1:t}, \mathbf{o}_{1:t}\right) = \prod_{i=1}^{B} p\left(s_{i,1:t} | \,\mathbf{o}_{i,1:t}\right) \quad (34)$$

where $\mathbf{o}_{t,1:t}$ are the quality measures related to the AN i. At this point, the estimation of each $s_{i,t}$ can be performed independently. Since the situation can only take two possible values, the grid-based method [43] provides the optimal recursion to compute the posterior distribution $p(\mathbf{s}_{i,1:t}|\mathbf{o}_{i,1:t})$. This approach can be viewed as a deterministic PF with as many particles as different values of the discrete vector to be estimated. Let us denote $\gamma_{k,i,t}$ the conditional probability at time t for AN i to be in situation k ($k = 0$ for LOS and $k = 1$ for NLOS), i.e.,

$$p\left(\mathbf{s}_{i,t} \,|\mathbf{o}_{i,1:t}\right) = \gamma_{0,i,t}\delta\left(\mathbf{s}_{i,t}\right) + \gamma_{1,i,t}\delta\left(\mathbf{s}_{i,t} - 1\right). \quad (35)$$

These probabilities can be updated following the prediction and update steps of a Bayesian estimator. The prediction equation is

$$\gamma_{k,i,t|t-1} = \sum_{m=0}^{1} \gamma_{m,i,t-1|t-1} p\left(s_{i,t} = k \,|s_{i,t-1} = m\right) \quad (36)$$

where the probabilities $p(s_{i,t} = k|s_{i,t} = m)$ are defined as in (15) or (17) (depending on the adopted model). The update equation is

$$\gamma_{k,i,t} \propto \gamma_{k,i,t|t-1} p\left(\mathbf{o}_{i,t} \,|s_{i,t} = k.\right) \quad (37)$$

resulting from the Bayes' rule. The problem of the normalizing constant can be solved by using the relationship $\gamma_{0,i,t} + \gamma_{1,i,t} = 1$. It should be noted that the same equations are obtained if considering the estimation problem as a Hidden MP (HMP) and solving it through forward iteration [44]. In the sequel, let us define the vector $\gamma_t \left[\gamma_{0,1,t} \quad \cdots \quad \gamma_{0,B,t}\right]$ containing the probabilities of being in LOS for all ANs. This vector characterizes completely the localization context since the LOS probabilities can be simply inferred as

$$\gamma_{1,i,t} = 1 - \gamma_{0,i,t}, \text{ for } i = 1, \ldots, B. \quad (38)$$

2) Conditional Estimation of the State Vector: We propose to use an UKF to obtain a Gaussian approximation of the pdf $p(\mathbf{x}_t|\mathbf{y}_{1:t}, \gamma_{1:t})$ and thus compute the state estimate as

$$\hat{\mathbf{x}}_t = E\left\{\mathbf{x}_t \,|\mathbf{y}_{1:t}, \boldsymbol{\gamma}_{1:t}\right\}. \quad (39)$$

The difficulty lies in the observation noise which prevents a direct implementation of the UKF. Indeed, assuming $\gamma_{1:t}$ is set to its estimated value, the observation noise pdf can be estimated as

$$\hat{p}\left(n_{i,t}\right) = \gamma_{0,b(i),t} p\left(n_{i,t}|s_{b(i),t} = 0\right) + \gamma_{1,b(i),t} p\left(n_{i,t}|s_{b(i),t} = 1\right) \quad (40)$$

where $b(i)$ is the AN associated with measure i. The expression (40) makes the computation of the sigma points associated with $\mathbf{n}_t$ a hard operation since $(\hat{p}\mathbf{n}_t)$ is time varying and not Gaussian. In order to simplify the procedure, the IUKF was proposed in [13]. A sigma set is formed with twice the number of sigma points, where half are related to the LOS situation and the other half are related to the NLOS situation. When transforming this extended sigma set to the related mean and covariance, the probabilities γ_t are used to assign a weight to each scenario.

The complete algorithm is described at Table VI where $\mathcal{U}$ is the sigma set associated with $\mathbf{u}_t$. $\mathcal{N}_{i,j}$ is the sigma point associated with $n_{i,j}$, i.e., the observation noise for AN j, when in situation i. If the RV is not Gaussian, the sigma point can be obtained by propagating a Gaussian random variable through a function that provides the desired random distribution at output. Thus, the IUKF feeds from the estimation γ_t at step (VI.1). The

TABLE VI
IUKF ALGORITHM

- Calculate the sigma set:
$$\left\langle \bar{\mathbf{x}}_{t-1}, \mathbf{Q}_{\mathbf{x}_{t-1}} \right\rangle \xrightarrow{UT} \boldsymbol{\mathcal{X}}_{t-1}$$
- Predict the state:
$$\boldsymbol{\mathcal{X}}_{t|t-1} = \mathbf{F}\boldsymbol{\mathcal{X}}_{t-1} + \boldsymbol{\mathcal{U}}$$
$$\boldsymbol{\mathcal{X}}_{t|t-1} \xrightarrow{UT^{-t}} \left\langle \bar{\mathbf{x}}_{t|t-1}, \mathbf{Q}_{\mathbf{x}_{t|t-1}} \right\rangle$$
- Predict the observation
$$\mathcal{Y}^{i,j}_{t|t-1} = g\left(\boldsymbol{\mathcal{X}}_{t|t-1}\right) + \gamma_{j,b(i),t|t-1}\mathcal{N}_{j,b(i)} \quad \text{(VI.1)}$$
$$\boldsymbol{\mathcal{Y}}_{t|t-1} = \begin{bmatrix} \mathcal{Y}^{1,1}_{t|t.1} & \mathcal{Y}^{1,2}_{t|t.1} \\ \vdots & \vdots \\ \mathcal{Y}^{N,1}_{t|t.1} & \mathcal{Y}^{N,2}_{t|t.1} \end{bmatrix} = \begin{bmatrix} \mathcal{Y}_{0,t|t-1} & \cdots & \mathcal{Y}_{4L_y+1,t|t-1} \end{bmatrix}$$
$$\boldsymbol{\mathcal{Y}}_{t|t-1} \xrightarrow{UT^{-1}} \left\langle \bar{\mathbf{y}}_{t|t-1}, \mathbf{Q}_{\mathbf{y}_{t|t-1}} \right\rangle \quad \text{(VI.2)}$$
- Obtain the Kalman Gain Matrix
$$\left\langle \boldsymbol{\mathcal{X}}_{t|t-1}, \boldsymbol{\mathcal{Y}}_{t|t-1} \right\rangle \xrightarrow{UT^{-t}} \mathbf{Q}_{\mathbf{xy}_{t|t-1}} \quad \text{(VI.3)}$$
$$\mathbf{K}_t = \mathbf{Q}_{\mathbf{xy}_{t|t-1}} \mathbf{Q}^{-1}_{\mathbf{y}_{t|t-1}}$$
$$\bar{\mathbf{x}}_t = \mathbf{x}_{t|t-1} + \mathbf{K}_t\left(\mathbf{y}_t - \bar{\mathbf{y}}_{t|t-1}\right)$$
$$\mathbf{Q}_{\mathbf{x}_t} = \mathbf{Q}_{\mathbf{x}_{t|t-1}} - \mathbf{K}_t \mathbf{Q}_{\mathbf{y}_{t|t-1}} \mathbf{K}_t^{-1}$$

UT presented at (VI.2) is double sized and described in [13]. The weights are the same as (52) considering $W_{i+2L+1} = W_i$ for $i > 2L+1$. The UT presented at (VI.3) is described in [40]. The presented approach has a computational cost similar to an EKF with NLOS mitigation capabilities and with the stability features associated to UKF. However, the RBPF is expected to outperform the IUKF algorithm since it does not consider the assumption of independence in the (34).

VI. SIMULATION RESULTS

This section presents some simulations results to compare the behavior of the proposed approaches to previous methods. The first simulation setting is highly detailed, in order to give the reader a better understanding of the concepts presented before. The proposed methods have been benchmarked to other positioning algorithms which are available in the literature. Some of them (like the ML) do not use any prior information regarding the unknown parameters and thus one can expect that these methods lead to lower performance. However, a comparison between Bayesian and non-Bayesian methods is interesting since it allows one to quantify the performance gain due to the use of prior information.

A. One BS With TOA and AOA Measures

The first battery of simulations reflects the case of having a BS as AN equipped with an antenna array. The BS is tri-sector, each one 120° wide. It is located at the origin of the system of coordinates. The MT moves at constant velocity. Both the MT and the BS are in the same horizontal plane, resulting in a two-dimensional motion environment. The rest of the simulation parameters are described in Table VII. These parameters have been chosen to reproduce a suburban scenario with an NLOS probability around 15%. The observation noise statistics for LOS and NLOS are provided in Table VIII. A particular realization of the observed TOA and AOA is depicted in Fig. 10. Fig. 8 represents

TABLE VII
SIMULATION 1 GLOBAL PARAMETERS

Parameter	Value
$E\{L_{LOS}\}$	30 m
$E\{L_{NLOS}\}$	5 m
MS speed	10 m/s
σ_v^2	1
Δt	0.01 s
Duration	200 s

The variance of the MT speed σ_v^2 is only considered for the UKF design, since actually the MT has constant speed.

TABLE VIII
SIMULATION 1 OBSERVATION NOISE DESCRIPTION

Measure	LOS		NLOS	
	Type	Variance	Type	Variance
TOA	Normal	10 m^2	Rayleigh	2000 m^2
AOA	Normal	10^{-5} rad^2	Normal	10^{-3} rad^2

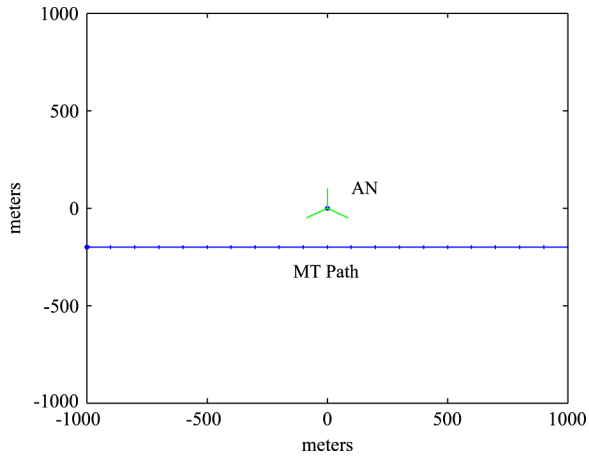

Fig. 8. MT and AN position for Simulation 1. The green lines departing from the BS are the sector frontiers. The crosses at the MS Path are placed at 10 s of time separation.

the position of the BS and the MT during the simulation. The orientation of the three sectors at the BS can also be observed. Although the MT velocity is constant, the transversal velocity to the BS is variable, leading to the LOS and NLOS situations shown in Fig. 9. The position computation functions used to estimate the MT position are detailed as follows.

- Maximum-Likelihood Estimator for LOS (**MLE-LOS**): Estimates the position only from the observations at the same time iteration, assuming they have been obtained under LOS conditions.
- **EKF-LOS**: A classical EKF is developed as in [37], assuming that all measures have been obtained in LOS situation.
- **IUKF**: The IUKF coupled to the situation estimator exposed in Section V-C.
- **RBPF + UKF**: The reordered RBPF with classical UKF, as exposed in Section V-B with $M = 8$.

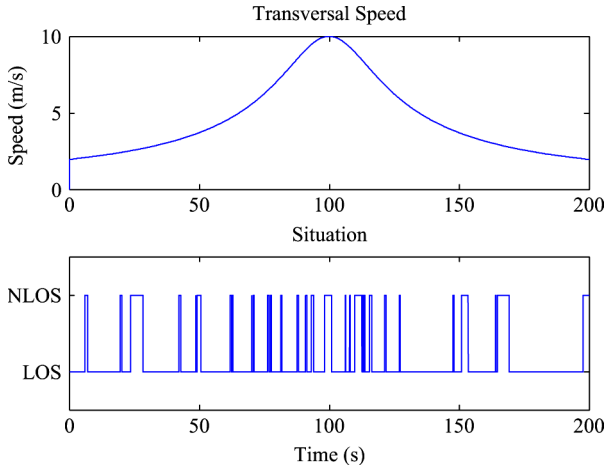

Fig. 9. Transversal speed and LOS-NLOS situation for one realization of Simulation 1. High transversal speed corresponds to high probability of situation change.

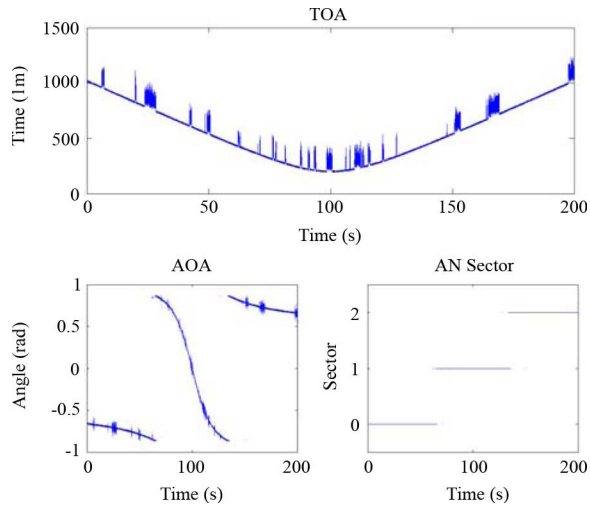

Fig. 10. Observation values for one realization of Simulation 1. The AOA is the electric angle. The discontinuities are changes of serving sector.

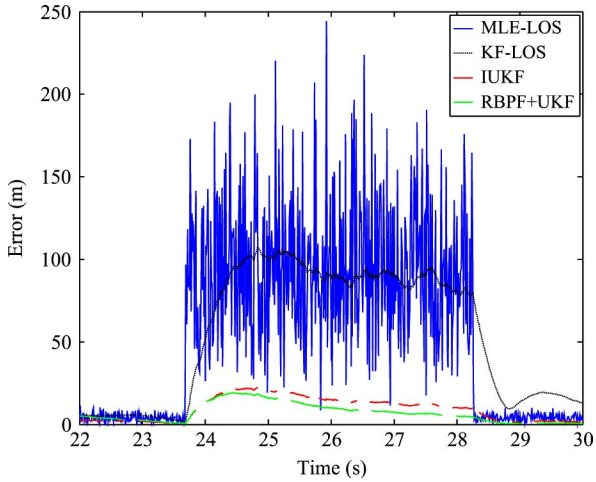

Fig. 11. Positioning error for different PCF inside a NLOS situation time frame.

Fig. 11 depicts one realization, focusing in an NLOS situation time frame. The MLE-LOS estimator is severely impaired by the high noise variances and biases due to the NLOS situation, since no tracking is performed. The EKF-LOS can cope with the high variances, but not with the introduced bias. The IUKF and the RBPF detect the NLOS situation, giving more weight to past measures than to new ones. Fig. 12 displays the situation estimation for both approaches for the same time interval. The effect of this estimation on the positioning accuracy can be observed in the positioning error cumulative distribution function (CDF) depicted in Fig. 13. The mean NLOS situation probability can be computed from (18) for this example: $p_N = 0.14$. The CDF of the MLE-LOS error is clearly bimodal, composed of two parts, one related with the LOS and the other with NLOS, with a probability equal to the mean situation probability. The EKF-LOS is affected by the NLOS situation with a higher probability, since the tracker takes time to converge when leaving the NLOS situation, contaminating LOS measures. Finally, the IUKF and the RBPF solutions exhibit a considerable gain in accuracy, both in LOS and NLOS. The difference between IUKF and RBPF is reduced, and the computational cost of RBPF is one order of magnitude larger. It can be concluded that the RBPF provides no considerable gain over the IUKF when only one AN is available.

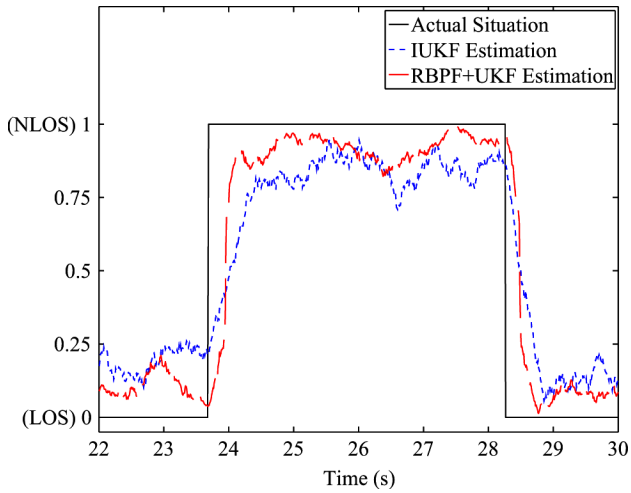

Fig. 12. Situation estimation for IUKF and RBPF approaches. Simulation 1.

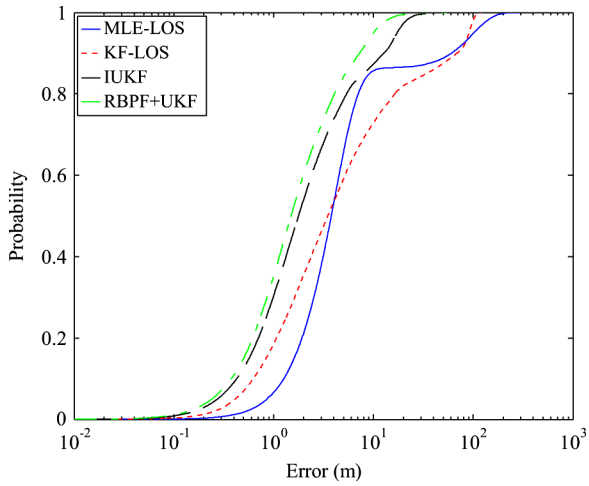

Fig. 13. CDF of the positioning error for different PCF obtained from 100 realizations of Simulation 1.

TABLE IX
SIMULATION 2 GLOBAL PARAMETERS

Parameter	Value
$E\{L_{LOS}\}$	10 m
$E\{L_{NLOS}\}$	10 m
σ_v^2	$1(\text{m/s})^2$
Δt	0.01 s
Duration	60 s
$E\{\tau_0^2\}$	$10\ \text{lm}^2$
$E\{\dot{\tau}_0^2\}$	$10\ (\text{lm/s})^2$
σ_τ^2	$10^{-2}(\text{lm/s})^2$

TABLE X
SIMULATION 2 OBSERVATION NOISE DESCRIPTION

Measure	LOS		NLOS	
	Type	Variance	Type	Variance
RTOA	Normal	10	Rayleigh	5000

B. Six ANs With RTOA Measures

Six ANs are placed forming a hexagon of 3-km side length. The MT departs from the center of the hexagon and follows a random walk based on parameters listed in Table IX. Each AN provides a RTOA measure at every time step. Thus, the clock skew has to be estimated. The clock skew and drift characteristics are summarized in Table IX. Table X provides the observation noise statistics. This scenario is urban with an NLOS probability of 50%. It means that more than 65% of the time there are not enough LOS ANs to perform a localization based only on LOS ANs.

The evaluated PCF are summarized as follows.

- **EKF-LOS**
- **CHEN**: The approach described in [10], where 50% of the combinations are rejected. The position estimator used for these combinations is an MLE whose implementation is based on simulated annealing [45].
- **CONG**: The Cong's approach has been described in [14]. The asymmetric Gaussian pdf is used to fit as likely as possible the Rayleigh distribution.
- **URR**: Urruela's approach based on a trellis search [17] which uses TDOA measures instead of RTOA ones.
- **IUKF**
- **cRBPF-128**: The RBPF/UKF approach is applied without the reordering as described in Section V-B ($M \times 2^B = 128$ UKF runs and $M = 2$ propagated particles through iterations).
- **rRBPF-16**: The reordered RBPF/UKF approach ($M = 16$ UKF runs and propagated particles).
- **rRBPF-128**: The reordered RBPF/UKF approach with $M = 128$ UKF runs and propagated particles.
- **PF**: A PF estimating both state and situation using (3). The PF uses 10^6 particles and the resampling is performed as for the RBPF, i.e., using the merging and selection strategies based on the distance measure (29).

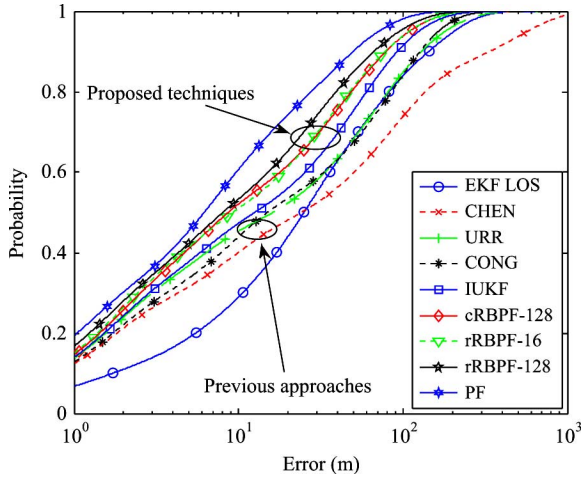

Fig. 14. Positioning error CDF for Simulation 2.

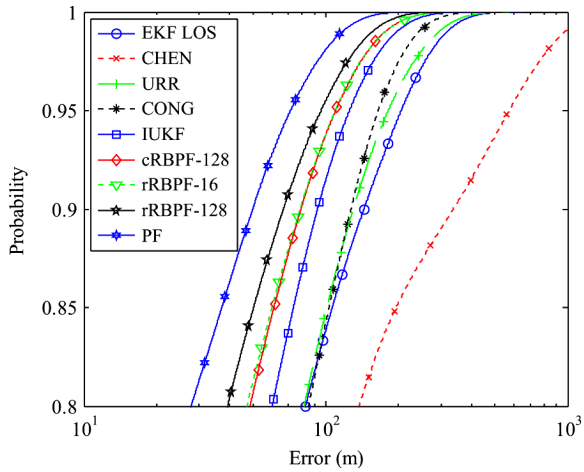

Fig. 15. Positioning error CDF for Simulation 2, zooming in around the 90% probability.

Note that some other approaches found in the literature do not seem to be useful for our problem. The algorithm proposed in [8] cannot be applied since it assumes constant bias. The idea developed in [19] has been discarded because it is based on geometrical information which has not been considered in the simulation tests. Finally, the algorithm proposed in [28] has not been considered since it is based on statistical information obtained online from a set of measurements.

Figs. 14 and 15 show the positioning error CDF for all considered position calculation functions. Since all ANs are in LOS during only 2% of the time, biased measures are virtually found all the time in the set of observations. The EKF-LOS behavior is severely impaired for this reason. CHEN, CONG, and URR approaches perform well in about 50% of time. However, the accuracy is degraded severely during the rest of the time. This behavior can be easily explained since these approaches require a minimum number of available ANs at LOS to achieve a good performance. In other words, these approaches are not suitable for strong NLOS environments. Note that the URR allows tracking, but in spite of this, does not outperform CONG mainly due to a noncharacterization of the NLOS observation noise.

The IUKF is the most inaccurate of all presented approaches. The high number of LOS/NLOS situation combinations degrades this simple estimator. Regarding the RBPF approaches, cRBPF-128 and rRBPF-16 show a similar behavior, while the rRBPF-16 is 16 times simpler than cRBPF-128. The variant rRBPF-128 (with the same complexity as cRBPF-128) shows a remarkably better behavior, demonstrating that the reordering strategy outstands the classical approach.

Finally, the PF approach achieves the best accuracy, but at the price of a prohibitive computational complexity. Indeed, the classical RBPF and the PF, with enough particles for each one, should perform the same if the model is actually conditionally linear Gaussian. The performance difference between the presented approach and PF comes from the suboptimal nature of UKF, which is avoided in PF providing enough particles are used.

VII. Conclusion

This paper addressed the radiolocation and tracking problem under NLOS situation. This problem is suitable for any radiolocation system such as GPS, Galileo, of cellular network based like GSM or UMTS. Two new robust approaches were developed to face the possible presence or absence of LOS offering a high degree of scalability in terms of accuracy and complexity. Both approaches jointly estimated the position and LOS/NLOS situation aided with quality measures. The first technique, based on a joint RBPF/UKF, achieved the best performance mainly due to an improved detection of LOS and NLOS situations (at the price of a computational cost lower than a PF-based solution). The second technique, based on a modification of the UKF, estimated the situation prior to the position computation. Its computational complexity is similar to the one obtained with a classical EKF (i.e., much reduced when compared to the joint RBPF/UKF approach) but is outperformed by the RBPF/UKF solution.

It should also be noted that the proposed approach could be used for GPS integrity monitoring in replacement of the classical algorithms dedicated to the detection of satellites failures which corrupt the pseudoranges.

The proposed approaches were tested under realistic urban scenarios with an associated high probability of NLOS situation. Such scenarios are well beyond the capabilities of classical NLOS mitigation strategies. The proposed navigation methodologies were developed for any combination of TOA, RTOA, TDOA, and AOA measures, and can be easily extended to other kind of measures, including MT mounted inertiometers.

Appendix

TDOA Versus RTOA Measures: One of the most common settings in localization systems consists of using a set of TOA observations with an unsynchronized MT (as for GPS). However, these measures are not strictly TOA observations since the transmission time is unknown by the MT. Because all measures are related to the same unknown transmission time, they will be called RTOA. Other works refer them to as pseudo-TOA [31] or pseudoranges.

Using a set of TDOA for this scenario allows avoiding the estimation of the clock skew, since it does not affect the TDOA measures. This property is confirmed by the analysis of the Cramer–Rao Bounds (CRB) of location estimation for TDOA and RTOA schemes (for unsynchronized MT) which are both equal [31]. Enhanced observation time difference and observed TDOA techniques have adopted the TDOA positioning because of this reason [5]. However, this is only true for a scenario without prior knowledge about position or clock skew.

This appendix studies a bound for the position estimation error with the aim of demonstrating that the RTOA approach outperforms the correlated TDOA when prior knowledge about clock skew is present (and hence justifies its use in this paper). Note that tracking the estimation of the clock skew can be translated into *a priori* knowledge for the next time interval.

Let us study the bound associated to RTOA when prior information on clock skew is available. The classical CRB is not suitable for estimators constructed with prior knowledge. Instead, we can use the Generalized CRB (GCRB) [46] (sometimes referred to as posterior CRB) defined by

$$E\left\{\left(\hat{\boldsymbol{\theta}}-\boldsymbol{\theta}\right)\left(\hat{\boldsymbol{\theta}}-\boldsymbol{\theta}\right)^{T}\right\}\geq \mathbf{J}^{-1} \tag{41}$$

where $\boldsymbol{\theta}\,[\,\mathbf{p}^T \quad \tau\,]^T$ is the vector to estimate and $\hat{\boldsymbol{\theta}}$ its estimation, $\mathbf{p}$ is the MT position and τ_0 the transmission time. In this case, the information matrix $\mathbf{J}$ is defined as

$$\mathbf{J}=\mathbf{J}_D+\mathbf{J}_P \tag{42}$$

where subscripts D and P stand for the *data* and *prior* components of the information matrix, respectively. The data information matrix expresses as

$$\begin{aligned}\mathbf{J}_D \triangleq\ & E_{\boldsymbol{\theta}}\left\{\left(\frac{\partial}{\partial\boldsymbol{\theta}}\ln f(\mathbf{y}|\boldsymbol{\theta})\right)\left(\frac{\partial}{\partial\boldsymbol{\theta}}\ln f(\mathbf{y}|\boldsymbol{\theta})\right)^{T}\right\}\\ &=\mathbf{H}_{\mathbf{y}/\boldsymbol{\theta}}\mathbf{Q}^{-1}\mathbf{H}_{\mathbf{y}/\boldsymbol{\theta}}^{T}\end{aligned} \tag{43}$$

where $\mathbf{y}$ is the set of TOA measures with pdf $f(\mathbf{y}|\boldsymbol{\theta})$, $\mathbf{Q}$ is its covariance matrix and $\mathbf{H}_{\mathbf{y}/\boldsymbol{\theta}}$ is defined as

$$\mathbf{H}_{\mathbf{y}/\boldsymbol{\theta}}=\frac{\partial\mathbf{y}}{\partial\boldsymbol{\theta}}=\begin{bmatrix}\cos\phi_1 & \cdots & \cos\phi_B\\ \sin\phi_1 & \cdots & \sin\phi_B\\ 1 & \cdots & 1\end{bmatrix}=\begin{bmatrix}\mathbf{H}_{\mathbf{y}/\mathbf{p}}\\ \mathbf{1}^T\end{bmatrix}. \tag{44}$$

The angles ϕ_t are the angles formed by the vectors linking the ANs and the MTs with respect to the X axis.

$$\begin{aligned}\mathbf{J}_P \triangleq\ & E_{\boldsymbol{\theta}}\left\{\left(\frac{\partial}{\partial\boldsymbol{\theta}}\ln f(\boldsymbol{\theta})\right)\left(\frac{\partial}{\partial\boldsymbol{\theta}}\ln f(\boldsymbol{\theta})\right)^{T}\right\}\\ &=\begin{bmatrix}0 & 0 & 0\\ 0 & 0 & 0\\ 0 & 0 & \sigma_\tau^{-2}\end{bmatrix}\end{aligned} \tag{45}$$

where σ_r^2 is the prior variance of the transmission time. Applying (43) and (45) in (42) yields

$$\mathbf{J}=\begin{bmatrix}\mathbf{H}_{\mathbf{y}/\mathbf{p}}\mathbf{Q}^{-1}\mathbf{H}_{\mathbf{y}/\mathbf{p}}^{T} & \mathbf{H}_{\mathbf{y}/\mathbf{p}}\mathbf{Q}^{-1}\mathbf{1}\\ \mathbf{1}^T\mathbf{Q}^{-1}\mathbf{H}_{\mathbf{y}/\mathbf{p}}^{T} & \mathbf{1}^T\mathbf{Q}^{-1}\mathbf{1}+\sigma_\tau^{-2}\end{bmatrix}. \tag{46}$$

The matrix block corresponding to the position (upper left 2×2 matrix) of the inverse of (46) is the GCRB of the position

$$E\left\{(\hat{\mathbf{p}}-\mathbf{p})(\hat{\mathbf{p}}-\mathbf{p})^H\right\} \geq \left[\mathbf{J}^{-1}\right]_{\mathbf{p}}. \quad (47)$$

Using standard results on inverses of block matrices [37, p. 572], the position GCRB can be expressed as

$$\begin{aligned}\left[\mathbf{J}^{-1}\right]_{\mathbf{p}} = &\mathbf{H}_{\mathbf{y}/\mathbf{p}}\mathbf{Q}^{-1}\mathbf{H}_{\mathbf{y}/\mathbf{p}}^T \\ &-\mathbf{H}_{\mathbf{y}/\mathbf{p}}\mathbf{Q}^{-1}\mathbf{1}\left(\mathbf{1}^T\mathbf{Q}^{-1}\mathbf{1}+\sigma_\tau^{-2}\right)^{-1}\mathbf{1}^T\mathbf{Q}^{-1}\mathbf{H}_{\mathbf{y}/\mathbf{p}}^T. \quad (48)\end{aligned}$$

It is straightforward to prove that $\left[\mathbf{J}_D^{-1}\right]_{\mathbf{p}} \geq \left[\mathbf{J}^{-1}\right]_{\mathbf{p}}$ in the sense that the difference matrix is semidefinite positive. Note that $\left[\mathbf{J}_D^{-1}\right]_{\mathbf{p}}$ is the CRB of the RTOA and TDOA cases without prior knowledge [31].

The conclusion is that prior knowledge about the transmission time improves the accuracy in the position when using RTOA measures. This conclusion cannot be extracted for TDOA since the transmission time does not affect the measures. The same conclusion applies when some of the measures are in NLOS [6]. So, since prior information over the clock skew is available in the presented approach, and in order to take advantage of the accuracy enhancement, the use of RTOA schemes is preferred to TDOA ones.

Sigma Points Spreading Strategy: Operator $\sqrt{\mathbf{A}}$ stands for the square root matrix of $\mathbf{A}$. Assume that vector $\mathbf{a}$ is a random variable with mean $\bar{\mathbf{a}}$ and covariance $\mathbf{Q}_{\mathbf{a}}$. The associated sigma set $\boldsymbol{\mathcal{A}}$ is a $(2L_{\mathbf{a}}+1) \times L_{\mathbf{a}}$ matrix where $L_{\mathbf{a}}$ is the length of $\mathbf{a}$. The columns of $\boldsymbol{\mathcal{A}}$, $\mathcal{A}_i$, are called sigma points and computed as

$$\begin{aligned}\mathcal{A}_0 &= \bar{\mathbf{a}} \\ \mathcal{A}_i &= \bar{\mathbf{a}} + \left(\sqrt{\alpha^2 L_{\mathbf{a}}\mathbf{Q}_{\mathbf{a}}}\right)\Big|_i \quad i = 1,\ldots,L_{\mathbf{a}} \\ \mathcal{A}_{i+L_{\mathbf{a}}} &= \bar{\mathbf{a}} - \left(\sqrt{\alpha^2 L_{\mathbf{a}}\mathbf{Q}_{\mathbf{a}}}\right)\Big|_i \quad i = 1,\ldots,L_{\mathbf{a}} \quad (49)\end{aligned}$$

where σ is a spreading factor normally of the order of 10^{-3}. The pass from the random vector to the sigma set is called UT and represented by

$$\langle \bar{\mathbf{a}}\mathbf{Q}_{\mathbf{a}} \rangle \xrightarrow{UT} \boldsymbol{\mathcal{A}}. \quad (50)$$

The statistics can be recovered from the sigma set by

$$\begin{aligned}\bar{\mathbf{a}} &= \sum_{i=0}^{2L} W_i^{(m)} \mathcal{A}_i \\ \mathbf{Q}_{\mathbf{a}} &= \sum_{i=0}^{2L} W_i^{(c)} (\mathcal{A}_i - \bar{\mathbf{a}})(\mathcal{A}_i - \bar{\mathbf{a}})^T \quad (51)\end{aligned}$$

where the weights are

$$\begin{aligned}W_0^{(m)} &= \frac{\lambda}{(L_{\mathbf{a}}+\lambda)} \\ W_0^{(c)} &= \frac{\lambda}{(L_{\mathbf{a}}+\lambda)} + 3 - \alpha^2 \\ W_i^{(m)} &= W_i^{(c)} = \frac{1}{(2L_{\mathbf{a}}+2\lambda)}, \quad i \neq 0 \\ \lambda &= \alpha^2 L_{\mathbf{a}} - L_{\mathbf{a}}. \quad (52)\end{aligned}$$

This operation is the inverse UT and represented by

$$\boldsymbol{\mathcal{A}} \xrightarrow{UT^{-1}} \langle \bar{\mathbf{a}}, \mathbf{Q}_{\mathbf{a}} \rangle. \quad (53)$$

REFERENCES

[1] F. Gustafsson and F. Gunnarsson, "Mobile positioning using wireless networks: Possibilities and fundamental limitations based on available wireless network measurements," *IEEE Signal Process. Mag.*, vol. 22, no. 4, pp. 41–53, Jul. 2005.

[2] A. Mihovska and J. M. Pereira, "Location-based VAS: Killer applications for the next-generation mobile internet," in *Proc. IEEE Int. Symp. Personal, Indoor and Mobile Radio Communications*, San Diego, CA, Sep. 2001.

[3] M. Silventoinen and T. Rantalainen, "Mobile station locating in GSM," in *Proc. IEEE Wireless Commun. Syst. Symp.*, Nov. 1995, pp. 53–59.

[4] D. N. Hatfield, "A Report on Technical and Operational Issues Impacting the Provision of Wireless Enhanced 911 Services," Federal Communications Commission, 2002.

[5] G. Sun, J. Chen, W. Guo, and K. J. R. Liu, "Signal processing techniques in network-aided positioning: A survey of state-of-the-art positioning designs," *IEEE Signal Process. Mag.*, vol. 22, no. 4, pp. 12–23, Jul. 2005.

[6] Y. Qi, H. Kobayashi, and H. Suda, "Analysis of wireless geolocation in a non-line-of-sight environment," *IEEE Trans. Wireless Commun.*, vol. 5, no. 3, pp. 672–681, Mar. 2006.

[7] S.-S. Woo, H.-R. You, and J.-S. Koh, "The NLOS mitigation technique for position location using IS-95 CDMA," in *Proc. IEEE Veh. Technol. Conf. Fall*, Boston, MA, Sep. 2000, pp. 2556–2560.

[8] M. P. Wylie and J. Holtzman, "The non-line of sight problem in mobile location estimation," in *Proc. IEEE Int. Conf. Universal Personal Commun.*, Cambridge, MA, Sep. 1996, pp. 827–831.

[9] Y. Qi and H. Kobayashi, "Cramer–Rao lower bound for geolocation in non-line-of-sight environment," in *Proc. IEEE Int. Conf. Acoust., Speech, Signal Process.*, Orlando, FL, May 2002, pp. 2473–6.

[10] P.-C. Chen, "A non-line-of-sight error mitigation algorithm in location estimation," in *Proc. IEEE Wireless Commun. Netw. Conf.*, 1999, pp. 316–320.

[11] "Recapitulation of the IPDL positioning method," Ericsson, Shin-Yokohama, Japan, 1999.

[12] S. Al-Jazzar, J. Caffery, Jr, and H.-R. You, "A scattering model based approach to NLOS mitigation in TOA location systems," in *Proc. IEEE Veh. Technol. Conf. Spring*, Birmingham, AL, May 2002, pp. 861–865.

[13] J. M. Huerta and J. Vidal, "Mobile tracking using UKF, time measures and LOS-NLOS expert knowledge," in *Proc. IEEE Int. Conf. Acoust., Speech, Signal Process.*, Philadelphia, PA, Mar. 2005, pp. 901–904.

[14] L. Cong and W. Zhuang, "Nonline-of-sight error mitigation in mobile location," *IEEE Trans. Wireless Commun.*, vol. 4, no. 2, pp. 560–573, Mar. 2005.

[15] J. Riba and A. Urruela, "A non-line-of-sight mitigation technique based on ML-detection," in *Proc. IEEE Int. Conf. Acoust., Speech, Signal Process.*, Montreal, QC, Canada, May 2004, pp. 153–156.

[16] A. Urruela and J. Riba, "Novel closed-form ML position estimator for hyperbolic location," in *Proc. IEEE Int. Conf. Acoust., Speech, Signal Process.*, Montreal, QC, Canada, May 2004, pp. 149–152.

[17] A. Urruela, H. Morata, and J. Riba, "NLOS mitigation based on a trellis search for wireless communications," in *Proc. IEEE Workshop Signal Process. Adv. Wireless Commun.*, New York, Jun. 2005, pp. 665–669.

[18] S. Venkatraman and J. Caffery, Jr, "A statistical approach to non-line-of-sight BS identification," in *Proc. Int. Symp. Wireless Personal Multimedia Commun.*, Honolulu, HI, Oct. 2002, pp. 296–300.

[19] S. Venkatraman, J. Caffery, Jr, and H.-R. You, "A novel TOA location algorithm using LoS range estimation for NLoS environments," *IEEE Trans. Veh. Technol.*, vol. 53, no. 5, pp. 1515–1524, Sep. 2004.

[20] B. L. Le, K. Ahmed, and H. Tsuji, "Mobile location estimator with NLOS mitigation using Kalman filtering," in *Proc. IEEE Wireless Commun. Netw. Conf.*, New Orleans, LA, Mar. 2003, pp. 1969–1973.

[21] J. M. Huerta and J. Vidal, "LOS-NLOS situation tracking for positioning systems," in *Proc. IEEE Workshop Signal Process. Adv. Wireless Commun.*, Cannes, France, Jul. 2006, pp. 1–5.

[22] B. Friedland, "Treatment of bias in recursive filtering," *IEEE Trans. Autom. Contr.*, vol. 14, no. 4, pp. 359–367, Aug. 1969.

[23] M. Najar, J. M. Huerta, J. Vidal, and J. A. Castro, "Mobile location with bias tracking in non-line-of-sight," in *Proc. IEEE Int. Conf. Acoust., Speech, Signal Process.*, Montreal, QC, Canada, May 2004, pp. 956–959.

[24] A. Giremus and J.-Y. Tourneret, "Joint detection/estimation of multipath effects for the global positioning system," in *Proc. IEEE Int. Conf. Acoust., Speech, Signal Process.*, Philadelphia, PA, Mar. 2005, pp. 17–20.
[25] A. Giremus, J.-Y. Tourneret, and V. Calmettes, "A particle filtering approach for joint detection/estimation of multipath effects on GPS measurements," *IEEE Trans. Signal Process.*, vol. 55, no. 4, pp. 1275–1285, Apr. 2007.
[26] J.-F. Liao and B.-S. Chen, "Robust mobile location estimator with NLOS mitigation using interacting multiple model algorithm," *IEEE Trans. Wireless Commun.*, vol. 5, no. 11, pp. 3002–3006, Nov. 2006.
[27] L. Cong and W. Zhuang, "Non-line-of-sight error mitigation in TDOA mobile location," in *Proc. IEEE Global Telecomm. Conf.*, San Antonio, TX, Nov. 2001, pp. 680–684.
[28] S. Al-Jazzar, J. Caffery, Jr, and H.-R. You, "Scattering-model-based methods for TOA location in NLOS environments," *IEEE Trans. Veh. Technol.*, vol. 56, no. 2, pp. 583–593, Mar. 2007.
[29] L. Garin, F. Van Diggelen, and J. Rousseaum, "Strobe and Enge correlator multipath rejection for code and phase carrier," in *Proc. ION 96*, Kansas City, MO, Sep. 1996, pp. 657–664.
[30] M. Brenner, "Navigation system with solution separation apparatus for detecting accuracy failures," U.S. patent 5,730,537, 1998.
[31] A. Urruela, J. Sala, and J. Riba, "Average performance analysis of circular and hyperbolic geolocation," *IEEE Trans. Veh. Technol.*, vol. 55, no. 1, pp. 52–66, Jan. 2006.
[32] L. E. Baum, T. Petrie, G. Soules, and N. Weiss, "A maximization technique occurring in the statistical analysis of probabilistic functions of Markov chains," *Ann. Math. Statist.*, vol. 41, no. 1, pp. 164–171, 1970.
[33] J. S. Liu, *Monte Carlo Strategies in Scientific Computing*. New York: Springer, 2001.
[34] P. M. Djurić, J. H. Kotecha, Y. Zhang, Y. Zhang, T. Ghirmai, M. F. Bugallo, and J. Miguez, "Particle filtering," *IEEE Signal Process. Mag.*, vol. 20, no. 5, pp. 19–38, Sep. 2003.
[35] A. Doucet, N. J. Gordon, and V. Krishnamurthy, "Particle filters for state estimation of jump Markov linear systems," *IEEE Trans. Signal Process.*, vol. 49, no. 3, pp. 613–624, Mar. 2001.
[36] E. Punskaya, A. Doucet, and W. J. Fitzgerald, "Particle filtering for joint symbol and code delay estimation in DS spread spectrum systems in multipath environment," *EURASIP J. Appl. Signal Process.*, vol. 2004, no. 15, pp. 2306–2314, Jun. 2004.
[37] S. M. Kay, *Fundamentals of Statistical Signal Processing: Estimation Theory Vol. 1*. Upper Saddle River, NJ: Prentice-Hall, 1993.
[38] M. Hellebrandt and R. Mathar, "Location tracking of mobiles in cellular radio networks," *IEEE Trans. Veh. Technol.*, vol. 48, no. 5, pp. 1558–1562, Sep. 1999.
[39] S. J. Julier and J. K. Uhlmann, "A new extension of the Kalman filter to nonlinear systems," in *Proc. Symp. Aerosp./Defence Sens., Simul. Contr.*, 1997, pp. 182–193.
[40] S. J. Julier and J. K. Uhlmann, "Unscented filtering and nonlinear estimation," *Proc. IEEE*, vol. 92, no. 3, pp. 401–422, Mar. 2004.
[41] S. J. Julier and J. K. Uhlmann, "Corrections to unscented filtering and nonlinear estimation," *Proc. IEEE*, vol. 92, no. 12, p. 1958, Dec. 2004.
[42] Y. Bar-Shalom, X. R. Li, and T. Kirubarajan, *Estimation with Applications to Tracking and Navigation*. New York: Wiley-Interscience, 2001.
[43] M. S. Arulampalam, S. Maskell, N. J. Gordon, and T. Clapp, "A tutorial on particle filters for online nonlinear/non-Gaussian Bayesian tracking," *IEEE Trans. Signal Process.*, vol. 50, no. 2, pp. 174–188, Feb. 2002.
[44] L. R. Rabiner and B. H. Juang, "An introduction to hidden Markov models," *IEEE Acoust., Speech, Signal Process. Mag.*, vol. 3, no. 1, pp. 4–16, Jan. 1986.
[45] S. Kirkpatrick, J. Gelatt, C. D. Gelatt, Jr, and M. P. Vecchi, "Optimization by simulated annealing," *Science*, vol. 220, no. 4598, pp. 671–680, May 1983.
[46] H. L. Van Trees, *Detection, Estimation and Modulation Theory*. New York: Wiley, 1968.

Jose M. Huerta received the Telecommunication Engineering degree from the Technical University of Catalonia (UPC), Barclona, Spain. He is currently pursuing the Ph.D. degree at UPC.

Since 2008, he has been a Software Quality, Security, and R&D Consultant at Palma de Mallorca, Mallorca, Spain. His research interest is in signal processing theory applied to radio-location.

Josep Vidal (M'91) received the Telecommunication Engineering and the Ph.D. degrees from the Technical University of Catalonia (UPC), Barcelona, Spain.

From 1989 to 1990, he was with the LTS at the Ecole Polytechnique de Lausanne. Since November 1996, he has been an Associate Professor at UPC. His current research interests are in statistical signal processing and information and communication theory. Since 2000 he has led UPC participation in the EC-funded projects, SATURN, FIREWORKS, ROMANTIK, and ROCKET. He has held research appointments with INP Toulouse and the University of Hawaii. He has authored more than 100 journal and conference papers in various areas of signal processing and communications.

Dr. Vidal was awarded the UPC's Premio Extraordinario de Doctorado.

Audrey Giremus received the Engineer degree and the Ph.D. degree in signal processing from SUPAERO (ENSAE), Toulouse, France.

She is currently an Associate Professor at the University of Bordeaux, Talence, France. Her research interests include statistical signal processing and optimal filtering techniques applied to navigation and localization.

Jean-Yves Tourneret (M'94–SM'08) received the Ingénieur degree in electrical engineering from Ecole Nationale Supérieure d'Electronique, d'Electrotechnique, d'Informatique et d'Hydraulique in Toulouse (ENSEEIHT), Toulouse, France, in 1989 and the Ph.D. degree from the National Polytechnic Institute, Toulouse, in 1992.

He is currently a Professor with the University of Toulouse, (ENSEEIHT) and a member of the IRIT Laboratory (UMR 5505 of the CNRS). His research activities are centered around statistical signal processing with a particular interest in Markov Chain Monte Carlo methods.

Dr. Tourneret was the program chair of the European conference on signal processing (EUSIPCO), which was held in Toulouse in 2002. He was also member of the organizing committee for the international conference ICASSP'06 which was held in Toulouse in 2006. He has been a member of different technical committees including the Signal Processing Theory and Methods (SPTM) committee of the IEEE Signal Processing Society (2001–2007). He is currently serving as an Associate Editor for the IEEE TRANSACTIONS ON SIGNAL PROCESSING.